

High-Performance Organohydrogel Artificial Muscle with Compartmentalized Anisotropic Actuation Under Microdomain Confinement

Longhao Zhang, Hao Yan, Jiajia Zhou, Ziguang Zhao, Jin Huang, Lie Chen, Yunfei Ru, and Mingjie Liu*

Current hydrogel actuators mostly suffer from weak actuation strength and low responsive speed owing to their solvent diffusion-induced volume change mechanism. Here a skeletal muscle-inspired organohydrogel actuator is reported in which solvents are confined in hydrophobic microdomains. Organohydrogel actuator is driven by compartmentalized directional network deformation instead of volume change, avoiding the limitations that originate from solvent diffusion. Organohydrogel actuator has an actuation frequency of 0.11 Hz, 110 times that of traditional solvent diffusion-driven hydrogel actuators ($<10^{-3}$ Hz), and can lift more than 85 times their own weight. This design achieves the combination of high responsive speed, high actuation strength, and large material size, proposing a strategy to fabricate hydrogel actuators comparable with skeletal muscle performance.

1. Introduction

Hydrogel actuators are regarded as promising candidates for muscle substitutions and biomedical applications^[1–4] owing to their unique softness, responsiveness, and biocompatibility. However, their performances such as responsive speed and actuation strength could be hardly compared with human skeletal muscle or elastomer actuators,^[5,6] and this disparity originates from their actuation mechanisms.^[7–9] Existing hydrogel actuators are mostly driven by solvent diffusion-induced volume change, thus possessing two characteristics: 1) the responsive

speed is correlated with solvent diffusion speed and further proportional to the square of material radius,^[10] restricting the fabrication of large-sized materials; 2) the actuation strength depends on the work done by deswelling, thus having a maximum value limited by swelling ratio.^[11] As a result, combinations of large material size, high responsive speed, and high actuation strength are difficult to achieve in a single hydrogel. In contrast, human skeletal muscles notably surpass hydrogel actuators in overall performance. Muscles are driven by a compartmentalized mode with high efficiency, that myofilaments sliding occurs in microresponsive units to generate force and deformation.^[12] This

mechanism relies on the oleophilic tissues named fascia^[13,14] to harmonize all responsive units, by the reason that fasciae can orientate their deformations and converge their output forces. Inspired by skeletal muscle, here we report an organohydrogel actuator (OHA) that combines oriented hydrophilic responsive network and oleophilic confinement network synergistically. In OHA, solvents can be confined inside hydrophobic microdomains, while actuations can be accomplished by the directional deformation of responsive network. Based on the mechanism, OHA exhibited a size-independent responsive speed of 0.11 Hz and actuation strength of 473 kPa, surpassing traditional hydrogels ($<10^{-3}$ Hz and 10^{-1} kPa). The volume phase transition process of OHA was analyzed by confocal laser scanning microscope (CLSM), small angle X-ray scattering (SAXS) and differential scanning calorimeter (DSC) microscopically. These characterizations reveal how oleophilic networks along with responsive networks confine solvents and achieve anisotropic actuation. We suppose our muscle-mimetic strategy could broaden existing driven mechanisms of hydrogel actuators, meanwhile breaking through their ceiling efficiency significantly.

2. Results and Discussion

With the development of hydrogel actuators, how to improve actuation performance has attracted broad attention. Current strategies mostly focus on the optimization of solvent diffusion process (Figure 1A), which dominates most hydrogel

L. Zhang, H. Yan, Z. Zhao, J. Huang, L. Chen, Y. Ru, M. Liu
Key Laboratory of Bioinspired Smart Interfacial Science and Technology
of Ministry of Education
School of Chemistry
Beihang University
Beijing 100191, P. R. China
E-mail: liumj@buaa.edu.cn

J. Zhou
South China Advanced Institute for Soft Matter Science and Technology
School of Molecular Science and Engineering
South China University of Technology
Guangzhou 510640, P. R. China

M. Liu
International Research Institute for Multidisciplinary Science
Beihang University
Beijing 100191, P. R. China

 The ORCID identification number(s) for the author(s) of this article can be found under <https://doi.org/10.1002/adma.202202193>.

DOI: 10.1002/adma.202202193

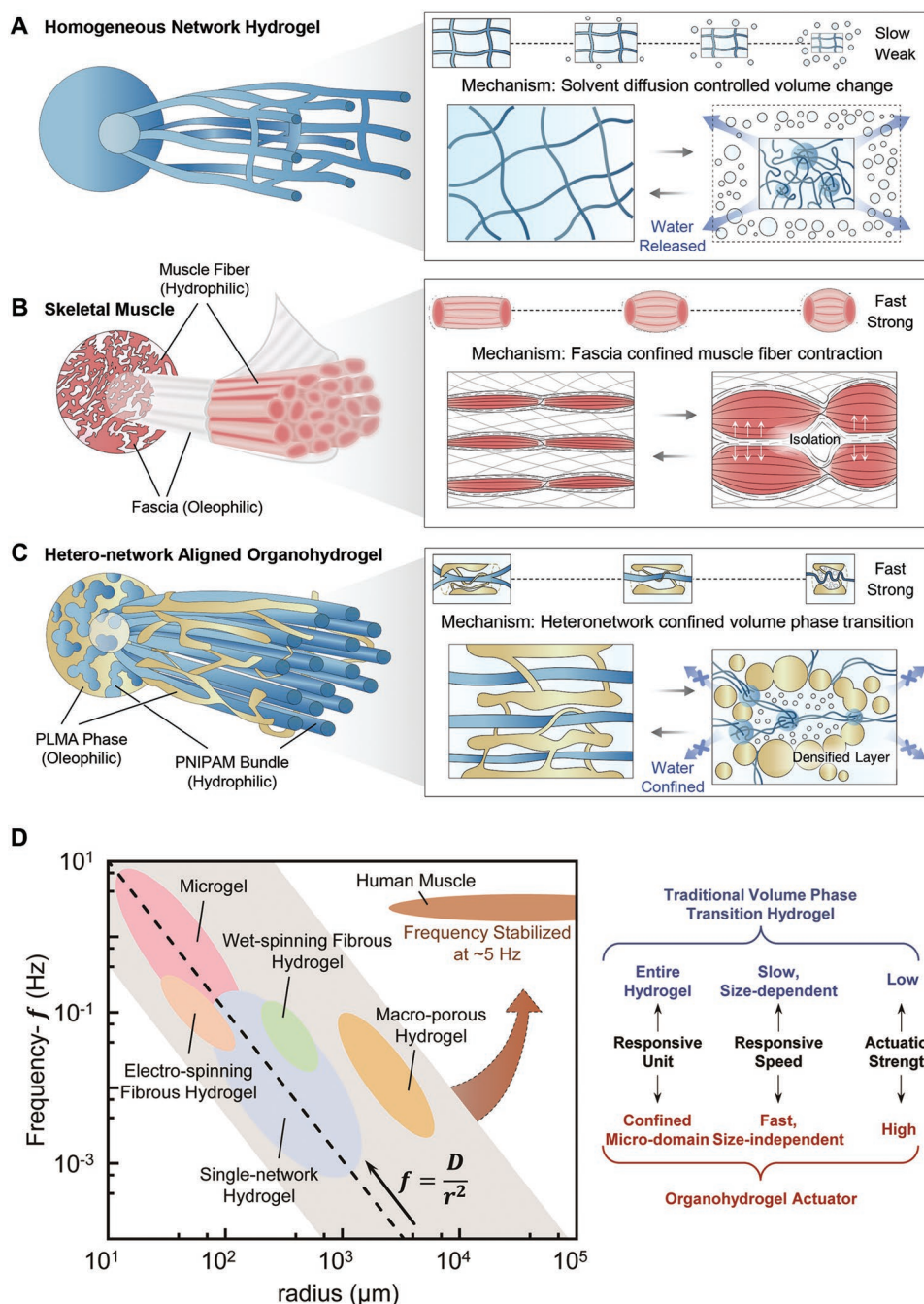


Figure 1. Design concept, mechanism, fabrication, and structure of organohydrogel actuators. A) Schematic of traditional homogeneous network hydrogel driven by solvent diffusion. B) Human skeletal muscle structure and myofibrils sliding mechanism, in which fascia isolate adjacent muscle fibers and confine their actuation direction. C) Structure of hetero-network aligned organohydrogel. The oleophilic network together with collapsed PNIPAM network form a densified layer to confine water movement, resulting in a network contraction-induced actuation mechanism independent with solvent diffusion. D) Traditional hydrogels comply with the rule that: responsive time is proportional to the square of material radius.

actuators, thus proposing methods such as constructing channels for solvents^[15,16] and reducing material size.^[17,18] Owing to their fixed actuation mechanism, however, these strategies are still troubled by low actuation strength or the tradeoff between responsive speed and material size. In fact, solvent diffusion-induced volume change is generally inevitable in hydrogel system, and it would become disturbance for hydrogel actua-

tors with mechanism besides volume change. For example, T. Aida and coworkers reported a thermal responsive hydrogel,^[4] which deforms rapidly based on anisotropic electrostatic repulsion instead of solvent diffusion-induced volume change. Although this hydrogel can elongate rapidly at the early heating stage, it would still contract slowly upon persistently heating because of solvent diffusion. Therefore, it has become

a challenge for hydrogel actuators that: how to control solvent diffusion in hydrogel actuators, and further adjust their actuation behaviors.

Human skeletal muscle, the representative of biological actuation tissues, has provided an excellent example for hydrogel actuator design. Muscles are composed of well-ordered hierarchical fibrous structures, and their actuations are based on large amounts of compartmentalized microresponsive units. Compared with hydrogels driven by overall solvent diffusion, compartmentalized actuation mode of muscle can significantly improve the speed and efficiency. High-speed myofibril sliding in responsive units could generate deformation and force, and their actuations could be harmonized by fascia (Figure 1B). The function of fascia can be concluded into three parts specifically:^[14] i) Isolation. Fasciae confine muscle fibers in a stable environment, separating them from surrounding water and holding their structure. ii) Integration. Fasciae orientate the direction of muscle fiber deformation, concentrating actuation force. iii) Energy storage. Fasciae are elastic tissues that can store elastic energy during contraction, and the energy will be subsequently released to assist muscle recovery. In general, the coordination of fascia and muscle fiber plays a key role in the high-performance actuation of muscle.

Mimicking the structure and actuation mechanism of skeletal muscle, we are supposed to adjust solvent diffusion in volume phase transition by the coordination of heterogenous network. Accordingly, an oleophilic network composed of poly (lauryl methacrylate) (PLMA) was interpenetrated into poly (N-isopropylacrylamide) (PNIPAM) hydrogel by amphiphilic solvent swelling method^[19] (Figure S1, Supporting Information). The obtained OHA contains an oriented hydrophilic network as a responsive unit, corresponding to myofibrils; and an elastic oleophilic network as a confinement network, corresponding to fascia (Figure 1C). Responsive PNIPAM networks undergo coil-to-globule transition when heated above the lower critical solution temperature (LCST), increasing the internal osmotic pressure and leading to deswelling.^[20,21] The collapsed PNIPAM networks form hydrophobic layers to hinder solvent diffusion, whereas they are not densified enough and are easily broken under osmotic pressure. In OHA, interpenetrated PLMA networks aggregate under the hydrophobic interaction in water, forming hydrophobic phases. We supposed PLMA phase along with collapsed PNIPAM can form a densified hydrophobic layer jointly,^[22] confining solvent diffusion in formed microdomain and enhance actuation performance. The responsive of traditional hydrogel actuators is correlated with volume change, thus complying with T. Tanaka mode: the responsive time of this process can be measured by the following formula: $\tau = r^2/D$.

Here τ refers to responsive time, r refers to material radius and D refers to solvent diffusion coefficient.^[10] When measured by actuation frequency ($\tau \cdot f = 1$), this formula can also be written as $f = D/r^2$. Current hydrogel actuators, such as electrospinning fibrous gel,^[17] wet-spinning fibrous gel,^[23] or macroporous gel,^[24,25] essentially improve actuation speed by changing solvent diffusion coefficient (Figure 1D). Consequently, problems that originate from solvent diffusion-induced volume change mechanism still exist, e.g., the trade-off between responsive speed and material size, low actuation speed. Conversely,

muscles exhibit stable high-speed, high-strength actuation at different sizes. OHA demonstrates a heteronetwork controlled compartmentalized mechanism mimicking muscle, achieving the combination of high-speed, high-actuation strength, and large material size. We also believe OHA can supply space for further hydrogel actuator performance improvements.

We characterized the actuation process of OHA to demonstrate its mechanism. The fabrication of OHA was briefly described below: PNIPAM hydrogel was first stretched, fixed, and dried. Afterward the sample was immersed in PLMA/ethanol pre-polymerized solutions for 12 h. The ethanol gel was polymerized, washed, and immersed in water to exchange solvent (Figure 2A). According to SEM and CLSM (Figure S2, Supporting Information) images, oleophilic network tend to fill the strip gaps formed by stretched PNIPAM networks, maintaining their orientation degree. To compare mechanism differences, an anisotropic double network hydrogel actuator (HA) was fabricated by a similar method. The orientation of PNIPAM networks was both kept in OHA and HA, the difference is that OHA was fixed by oleophilic PLMA while HA was fixed by hydrophilic polyacrylamide (PAM). We suppose hydrophilic networks in HA could not form confined microdomains to limit solvents, retaining the volume change mechanism. To clearly describe all samples, the nomenclature for OHA or HA with different network ratio and the stretched ratio is marked as OHA(HA)_{X-Y-R}. Here X refers to the fixed network weight ratio, Y refers to the responsive network weight ratio and R refers to the stretched ratio, e.g., OHA_{0.8-1.0-4}. Before the test of responsive speed, OHA and HA samples were heated (for 60 s) and cooled (for 60 s) circularly till balanced, then immersed in water (R.T.) for 5 min. The tested sample was hung in two-way glass tubes during measurement, then hot water (60 °C) and cold water (15 °C) were poured alternately to control environment temperature. Results show that OHA_{0.8-1.0-4} exhibits a contraction process of 3.2 s ± 0.5 s and an elongation process of 6.0 s ± 0.9 s (Figure 2B; Figure S4, Supporting Information), while HA_{0.8-1.0-4} exhibits a much lower speed (contraction process of 60 s ± 10 s, elongation process of 360 s ± 30 s, Figure S5, Supporting Information). OHA and HA also exhibit similar strain (10.7 ± 1.6% for OHA_{0.8-1.0-4}, 12.5 ± 1.7% for HA_{0.8-1.0-4}). Meanwhile, HA shows an obvious feature of solvent diffusion-driven hydrogels, that the speed of elongation is several times higher than contraction, that $t_{\text{elongation}}/t_{\text{contraction}} \approx 6$. In contrast, OHA has a much lower value that $t_{\text{elongation}}/t_{\text{contraction}} \approx 1.9$. OHA has also showed a stable periodic actuation behavior at high speed (Figure S14, Supporting Information). Above experiments demonstrated the significant differences in responsive speed and $t_{\text{elongation}}/t_{\text{contraction}}$ ratio between OHA and HA, which we supposed originate from the mechanism. We then adjusted the ratio of hetero-network in OHA, investigating its influence on responsive speed and strain (Figure 2C). From OHA_{0.2-1.0-4} to OHA_{2.0-1.0-4}, their actuation frequencies increased from 2×10^{-3} to 2×10^{-1} Hz with increasing of oleophilic network. The improvement of responsiveness was established on the sacrifice of actuation strain, which decreased from 15.5% (for OHA_{0.2-1.0-4}) to 7% (for OHA_{2.0-1.0-4}) correspondingly. In comparison, HA_{0.8-1.0-4} was accompanied by responsive speed (2×10^{-3} Hz) much lower than all OHA samples. We suppose the increased responsive speed of OHA originates from the

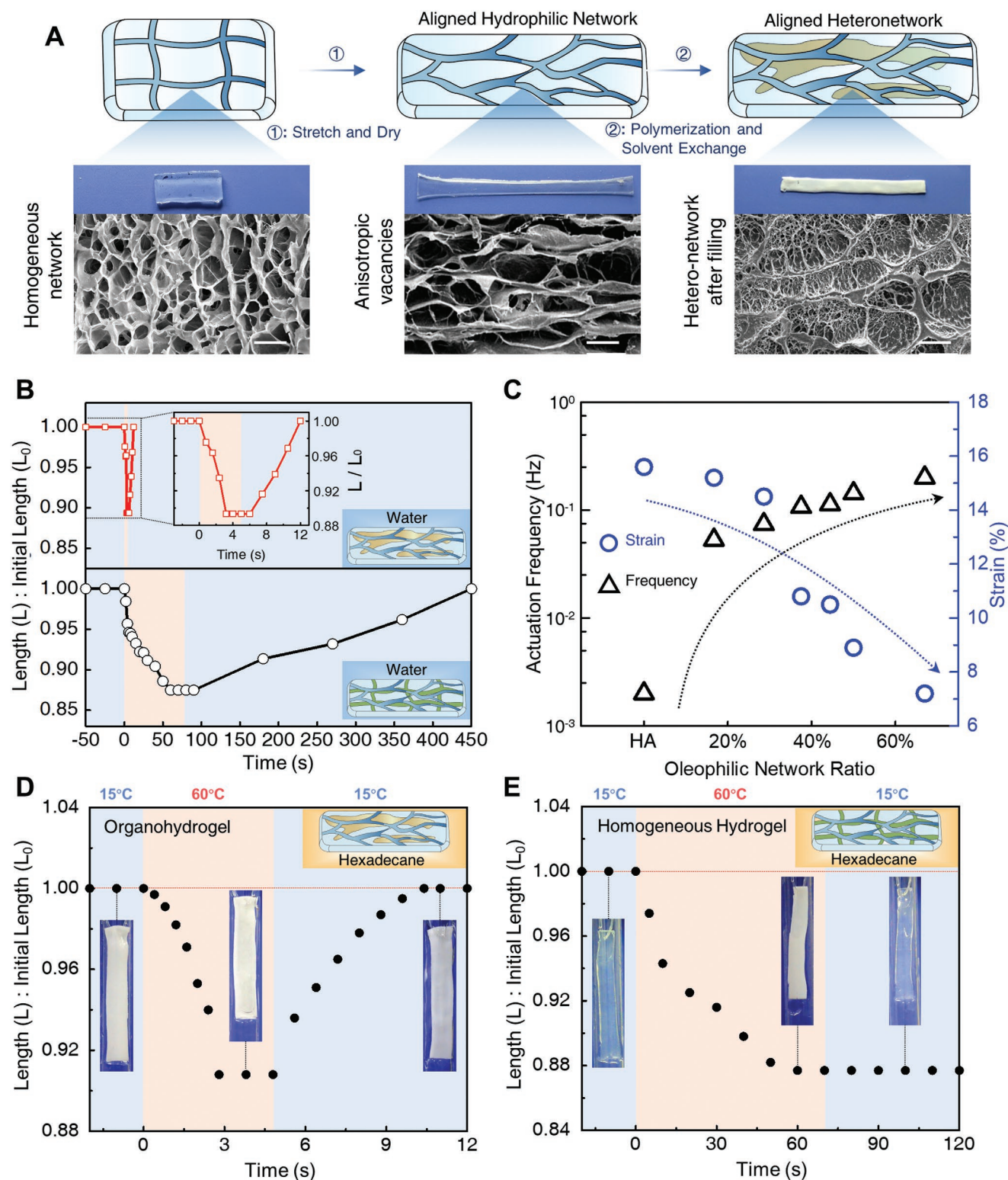


Figure 2. Actuation speed and strain of OHAs. A) The fabrication process and SEM images corresponding to each step. SEM images for each step were characterized from samples after freeze drying, scale bar is 25 μ m. B) Comparison of OHA and HA actuated in water environment. C) Actuation frequency and strain of OHAs tested at oleophilic network ratio of 16.7%, 28.6%, 37.5%, 44.4%, 50%, and 66% D) OHA and E) HA actuated in *n*-hexadecane from 15 to 60 °C.

difference between directional network deformation and solvent diffusion-induced volume change, whereas excess oleophilic networks may limit PNIPAM network contractions and reduce their strain.

To directly prove the mechanism we proposed, the actuation of OHA and HA were repeated in non-water environment, and that heating and cooling solvent was changed to *n*-hexadecane. Since hydrogels swelling were prevented in *n*-hexadecane, they cannot accomplish actuation when driven by volume change. Results show that OHA still exhibits actuation behavior analogous to the water environment, that OHA_{0.8-1.0-4} has contraction process of 2.8 ± 0.7 s, elongation process of 5.6 ± 0.9 s, and strain of $= 9.2\% \pm 0.6\%$ (Figure 2D; Figure S6, Supporting Information). The stable periodic actuation was also repeated in *n*-hexadecane (Figure S18, Supporting Information). HA can only contract at a similar speed, but cannot recover to its initial length after cooling (Figure 2E). These results indicate that the recovery of HA relies on swelling while the recovery of OHA is not. Another comparison experiment of OHA_{0.8-1.0-1} and OHA_{0.8-1.0-4} indicates that only anisotropic samples can exhibit deformation when temperature changes (Figure S7, Supporting Information), consistent with our theory that OHA actuations rely on directional network deformation. Here we summarize the functions of oleophilic network in two parts: i) confine solvents in microdomains, promoting responsive speed. ii) maintain anisotropic PNIPAM network, assisting their directional network deformation. The actuation process can be regarded as powerful evidence for the confinement anisotropic actuation mechanism of OHA.

The new mechanism of OHA also leads to the increase of actuation strength. We first investigate the mechanical strength of OHA at room temperature. We fabricated tensile bars with various network ratios, then the samples were subjected to tensile test (rate of 10 mm min^{-1} , temperature of $25 \text{ }^\circ\text{C}$). The stress-strain curves (Figure 3A) display that the fracture stress of OHA is proportional to oleophilic network content, with fracture strength increase from 0.4 ± 0.06 MPa of OHA_{0.2-1.0-4} to 0.8 ± 0.09 MPa of OHA_{2.0-1.0-4}. As a trade-off, their strains decrease from 3.5 ± 0.3 of OHA_{0.2-1.0-4} to 2.0 ± 0.2 OHA_{2.0-1.0-4}. These results suggest that elastic oleophilic network can enhance mechanical strength while sacrifice strain when interpenetrated with PNIPAM. We then investigated the actuation strength of OHA by isometric contraction model,^[26] which originates from muscle test. Specifically, the output force of muscle is proportional to bearing load (Figure S8, Supporting Information), and the output force increase with load till the sample cannot contract. Analogously, the actuation strength of OHAs reach a maximum value at a fixed length, and this value can be regarded as the index for actuation strength. All tested samples were pre-treated as described in responsive speed test, then fixed by two clamps with constant distance and hung under the force meter (Figure 3B). The tested sample was immersed in hot water ($60 \text{ }^\circ\text{C}$) to initiate phase transition. It is observed that actuation strength increases along with stretched ratio for OHAs and stretched PNIPAM hydrogels, while the actuation strength of HA is lower than 10 kPa at all stretched ratio (Figure 3C). Stretched PNIPAM exhibits high actuation strength, increasing from 5.41 to 45.0 kPa along with stretched ratio increase from 1 to 6 . However, the stretched

PNIPAM hydrogels are not stable without fixing, and they can only demonstrate the function of anisotropic responsive network. The actuation strength of OHA increases from 8.0 kPa of OHA_{0.8-1.0-1} to 47.3 kPa of OHA_{0.8-1.0-5}, then fall back to 35.3 kPa when stretched ratio is six. We suppose this phenomenon happens due to the fracture of PNIPAM network at a high stretched ratio. The actuation of HA is based on volume change, thus exhibit a deswelling-induced low actuation strength in spite of high stretched ratio. These results indicate directional network deformation of responsive network can generate actuation strength much higher than deswelling, thus the alternative of mechanism becomes the key to actuation strength improvement. OHA provides an example to exclude the disturbance of solvent diffusion and exhibit high actuation strength.

We investigated the influence of oleophilic network ratio or stretched ratio to actuation strength. After being immersed in hot water ($60 \text{ }^\circ\text{C}$), all samples rapidly went to maximum actuation strength, subsequently decreasing slowly due to polymer relaxation. Figure 3D demonstrates a result similar to Figure 3C, revealing the highest actuation strength could be obtained at highest stretched ratio before fracture. Figure 3E shows the actuation strength of OHA exhibits an increasing trend from 21.7 kPa of OHA_{0.2-1.0-5} to a maximum 47.3 kPa of OHA_{0.8-1.0-5}, next a decreasing trend to 16.8 kPa of OHA_{2.0-1.0-5}. Above experiments demonstrate the actuation strength originates from anisotropic network, and oleophilic network ratio influences the ability of maintaining orientation. OHA with low oleophilic network ratio is difficult to maintain the orientation of PNIPAM, resulting in a decrease of actuation strength. Oleophilic network could also orientate the responsive network deformation, concentrating actuation strength. However, the excess oleophilic network also hinders the contraction of responsive network. OHA_{0.8-1.0-5} presents the best actuation strength (47.3 kPa , Figure 3F), whereas we found this sample is not stable: its actuation force will decrease when used for several cycles. Conversely, OHA_{0.8-1.0-4} presents a stable periodic actuation behavior with similar actuation strength (Figure 3G; Figure S13, Supporting Information), thus is applied in responsive speed test and demonstrations. The periodical actuation experiment was conducted as method briefly described below: an OHA fiber was placed inside an electrothermal coil, and control the temperature by on-off switching voltage. OHA achieves the combination of high actuation strength and high speed comparable with muscle, and its comprehensive performance surpasses all existing hydrogel actuators (Figure 3H).

How does an oleophilic network change the actuation mechanism? We designed a series of characterizations to find the role of oleophilic network in phase transition. We first dyed the hydrophilic network by N-(1-Naphthyl)-3-aminopropanesulfonic acid sodium salt (ANSA) as previously reported,^[27] and dyed oleophilic network by copolymerized with 1-pyrenylmethyl acrylate (PyMA). As a result, the heteronetworks were marked respectively. CLSM images demonstrate the structure of heterogenous network at microscale, indicating oleophilic network undergoes shape change from strip (length ranging from $10\text{--}100 \text{ }\mu\text{m}$, width ranging from 1 to $20 \text{ }\mu\text{m}$) at $15 \text{ }^\circ\text{C}$, to globule (diameter ranging from 1 to $30 \text{ }\mu\text{m}$) at $60 \text{ }^\circ\text{C}$ (Figure 4A; Figure S10, Supporting Information). Considering the strain difference between macroscopic OHA and strip to a globule,

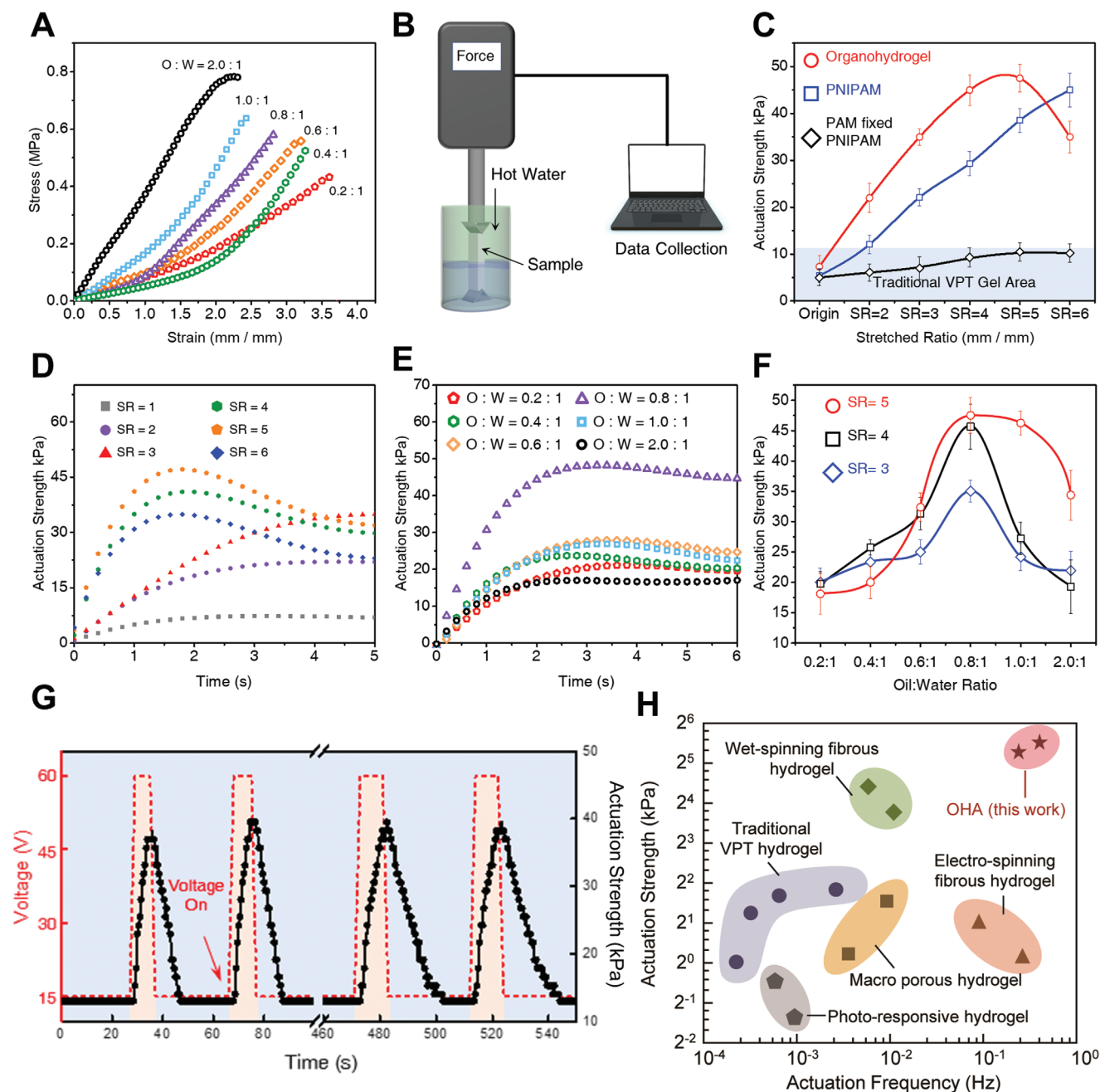


Figure 3. Actuation strength of OHAs. A) Tensile stress–strain experiment of OHAs, tested at speed of 10 mm min^{-1} , $25 \text{ }^\circ\text{C}$. B) Schematic of testing device for isometric model. C) Actuation strength with a stretched ratio range from 1 to 6 of organohydrogel, pure PNIPAM gel, and double network VPT gel, which are heated to $60 \text{ }^\circ\text{C}$ rapidly by hot water. Actuation strength curves of D) stretched ratio and E) network ratio. F) Actuation strength varies with stretched ratio and oleophilic to hydrophilic network ratio. G) Periodical output of OHA, actuated by electrical heating tube with voltage from 0 to 60 V. H) Comparison of actuation strength and actuation frequency of organohydrogel, wet spinning fiber, electrospinning fiber, light responsive gel, and VPT gel.

the conformation change of oleophilic phase probably originates from PNIPAM division during aggregation. The CLSM image at $60 \text{ }^\circ\text{C}$ exhibits a low oleophilic network ratio, which was supposed to be covered by PNIPAM network according to the pure oleophilic network image in Figure S10 (Supporting Information). Moreover, uniform globule structure at high temperature indicates that: the oleophilic phase was separated

by water and aggregated PNIPAM network. We further demonstrate the nanoscale structure by SAXS characterization, finding that oleophilic phase exhibit a distance of $\approx 15 \text{ nm}$ both at 15 and $60 \text{ }^\circ\text{C}$ (Figure S20, Supporting Information). Here we propose our hypothesis that: densified network forms a hydrophobic layer at the nanoscale, confining free water inside. Water motions were transformed from long-range diffusion

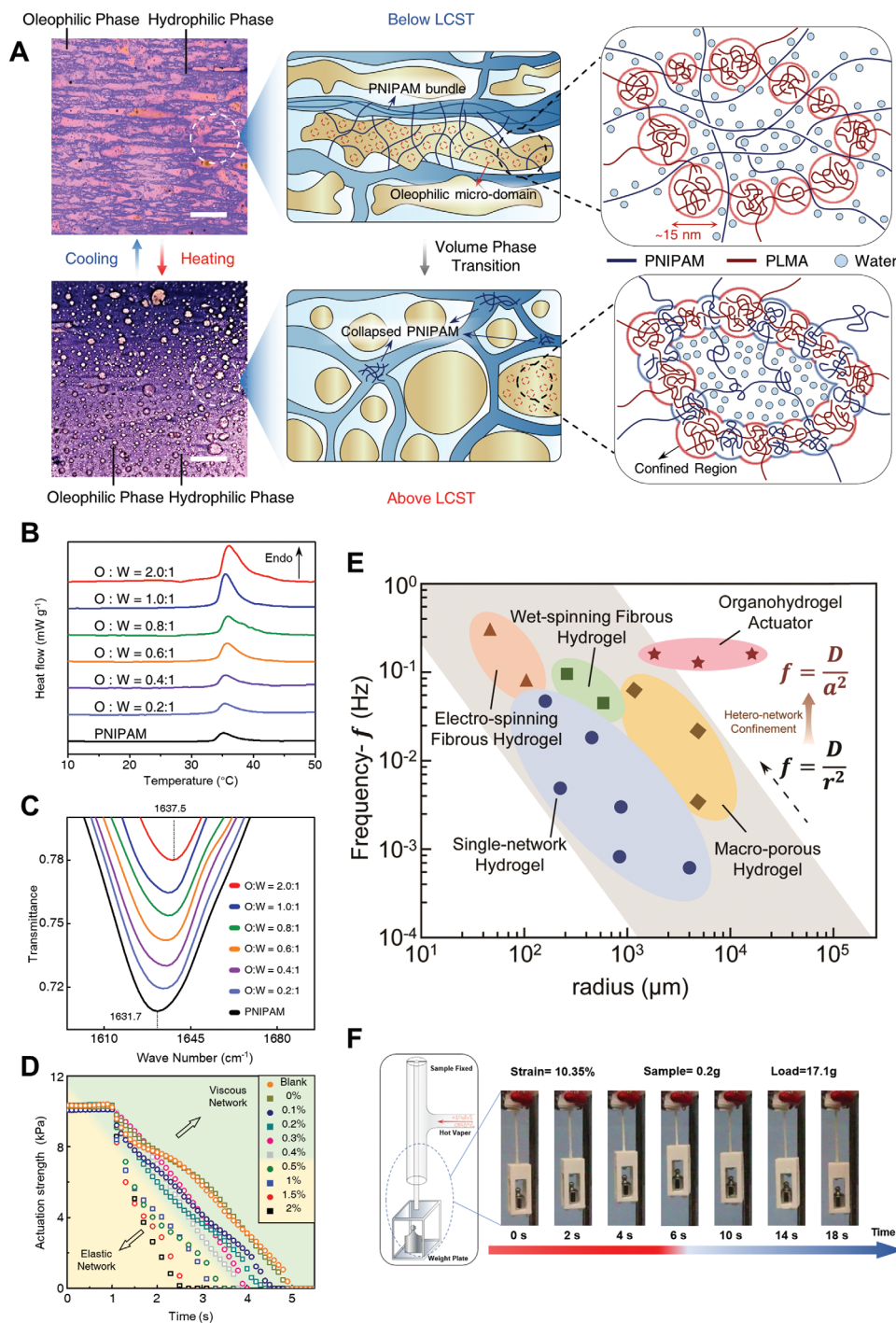


Figure 4. Mechanism analysis of OHA phase transition process in soft confinement environment. A) The CLSM images and network structure illustration are between 15 and 60 °C, scale bar is 50 μm. B) DSC measurement of OHAs and PNIPAM, heating from 15 to 50 °C at the rate of 5 °C min⁻¹. C) ATR-FTIR spectrum of OHAs at 25 °C. D) Recovery of actuation strength of organohydrogel containing elastic or viscosity oleophilic network. E) Performances comparison between OHA and current hydrogel actuators. F) Demonstration of actuation process, heating and cooling by water vapor.

across network into short range deformation inside domain.^[28] Figure 4B display that the endothermic peak area is proportional to the oleophilic network content, and we illustrate this phenomenon by PNIPAM contraction theory in diluted solutions.^[29] According to previous research, PNIPAM chains have two modes during phase transition (Figure S11, Supporting

Information): i) adjacent network aggregation, which is formed by inter-chain H-bond. ii) single chain folding, which is formed by intra-chain H-bond. Mode (i) is more stable than (ii), and corresponds to smaller endothermic peak area in differential scanning calorimetry (DSC). On the basis of stability difference, PNIPAM networks tend to aggregate during phase separation,

whereas contact of PNIPAM chains in OHA will be hindered by oleophilic network. Therefore, the ratio of intra-chain contraction will increase in OHA, leading to the increase of ΔH . This phenomenon also provides an explanation of why oleophilic network can concentrate actuation force: the directions of PNIPAM network contraction are also confined by oleophilic network. The Fourier transform infrared (FTIR) spectroscopy of OHA at 25 °C showed an evident blue shift of C=O peaks when increasing oleophilic network ratio (Figure 4C). OHA_{2.0:1.0} (oleophilic network: hydrophilic network) has a peak position at 1637.5 cm⁻¹, and PNIPAM has peak position at 1631.7 cm⁻¹. This result indicates the interaction between networks was enhanced by increasing oleophilic network, proving that PLMA networks are close enough to reduce the contact of PNIPAM networks. More oleophilic networks inserted into PNIPAM can enhance the confinement effect and promote the conformation change of PNIPAM. We then adjust the crosslink density of oleophilic network to investigate the influence of network elasticity. Rheological measurement (Figure S21, Supporting Information) suggests that PLMA elastomer storage modulus (G') and loss modulus (G'') varies with crosslink density (CD). When $G' > G''$ (corresponding to 0.5% < CD < 2%), PLMA displays an elastic state, which can recover after being compressed. When $G' < G''$ (corresponding to 0.1% < CD < 0.5%), PLMA displays a viscous state, which deforms as external force. Hot contracted samples were subjected to devices and cooled to measure the actuation strength curves in the elongation stage (Figure 4D). We observed the elongation speed of OHA with elastic network (< 3.7 s) is evidently higher than OHA with viscous network (>3.9 s). The results indicate that elastic oleophilic network can store energy when compressed by PNIPAM, while the elastic energy is dissipated in viscous network. The stored energy will be later released to accelerate elongation process analogous to fascia behavior.

Owing to the mechanisms above, OHA can exhibit high-speed actuation with good stability and various material size (Figure 4E). We suppose OHA complies with a new formula that: $f = D/a^2$. Here a refers to the size of micro-hydrophobic domain instead of macro-material size. Since the radius of microdomain only depends on the interaction between the heterogeneous network and solvent, they provide stable responsive speed at different material sizes. OHA also exhibits a responsive speed higher than most hydrogel actuators (Figure 4E). Utilizing the characterizations including high actuation strength and high speed of OHA, we further design an actuator as a demonstration. OHA fiber (mass = 0.2 g, length = 11.5 cm) is utilized as the actuation material with a load of 17.1 g. Actuation was induced by hot or cold vapor (Figure 4F; Figure S12, Supporting Information). Results show that OHA could lift load 85 times of own weight circularly (18 s for one cycle) in air environment.

3. Conclusions

We have fabricated a high-speed, high-actuation strength, large-sized gel actuator by incorporating heterogeneous networks. The soft confinement effect of oleophilic networks can be summarized into three parts: i) confine solvents in the micro-

domain by forming a hydrophobic densified layer, transforming water motions from long-range to short-range. ii) orientation of the deformation of PNIPAM network, concentrating actuation force directionally. iii) store elastic energy to assist the elongation process. We believe the network deformation mechanism of OHA can provide more space for actuation performance improvements, broadening the application range of hydrogel actuators.

4. Experimental Section

Materials: Reagents including *N*-isopropylacrylamide (NIPAM, 98%, GC), lauryl methacrylate (LMA, 95%, GC), 2-hydroxyethyl methacrylate (HEMA, 95%), 4-dimethylaminopyridine (DMAP, 99%), 1-pyrene butyric acid (98%) was purchased from Tokyo Chemical Industry (TCI) and used as received. Acrylamide (AM), ethylene glycol dimethacrylate (EGDMA, 99%), 2,2-diethoxyacetophenone (DEOP, 98%), *N,N'*-methylene bisacrylamide (BIS), 4',6-diamidino-2-phenylindole dihydrochloride (DAPI) were purchased from Sigma-Aldrich and used as received. 1-Ethyl-3-(3-dimethylaminopropyl) carbodiimide hydrochloride (EDCL, 98%), *N*-(1-naphthyl)-3-aminopropanesulfonic acid sodium salt (ANSA) and solvents including ethanol, acetone, dichloromethane were purchased from Aladdin Biomedical Technology Company. Inorganic nanoclay (Laponite XLS, [Mg₅34Li_{0.66}Si₈O₂₀(OH)₄] Na_{0.66}, MW = 762.24, layer size = 20–30 nm in diameter and 1 nm in thickness) was purchased from Rockwood Ltd., UK. (Laponite is a trademark of the company BYK Additives Ltd).

Synthesis of PNIPAM Hydrogels: Laponite XLS was first dispersed in water forming an 8 wt.% solution. Pre-polymerized solution was prepared by mixing 2.5 g of NIPAM (monomer), 7 mg of DEOP (photoinitiator), and 10 mL Laponite XLS nanoclay (cross-linker) solution. The thoroughly mixed solution was poured into a glass mold, which was placed in ice water after being sealed. The hydrogel was then synthesized by UV photoinitiated polymerization (365 nm) for 30 min at 0 °C. The obtained hydrogel was washed with deionized water three times, and stored at 5 °C for later use.

Orientation and Drying of PNIPAM Hydrogels: PNIPAM hydrogel was stretched to a specific ratio and fixed on a plastic board by clamps, then placed at room temperature for 12 h until dried. The obtained transparent sample was washed with acetone and dried three times to remove water completely. The weight of dried sample was measured and marked as m_{HN} (HN refers to hydrophilic network).

Synthesis of the Organohydrogel Actuator: Pre-polymerized solution was prepared by mixing LMA (monomer), DEOP (photoinitiator), EGDMA (cross-linker), and 100 mL of ethanol (solution). The concentration of DEOP was 0.01 wt%, and concentration of EGDMA was 0.5 wt% (both were the mass fraction of LMA). Dried PNIPAM was swelled with prepared solution (in fixed state) for 4 h at a cool, dark place. Obtained thoroughly swelled PNIPAM was polymerized by UV (365 nm) for 30 min at room temperature. The sample was washed with ethanol and water alternately three times to remove unreacted monomers, then swelled in water for 12 h (change water at least three times) until the exchanged solvent was completely. To measure m_{ON} (ON refers to oleophilic network), sample should be dried and weighed after washed and before swelled in water, and m_{ON} can be calculated as Equation (1):

$$m_{ON} = m_{\text{measured}} - m_{HN} \quad (1)$$

where m_{ON} and m_{HN} are utilized to measure oleophilic to hydrophilic network ratio. OHA was a store at 5 °C for later use.

Synthesis of HA Fixed with Hydrophilic Network: Pre-polymerized solution was prepared by mixing AM (monomer), DEOP (photoinitiator), BIS (cross-linker), and 100 mL of water. Mass fractions of DEOP and BIS are 0.01 and 0.5 wt.% correspondingly. The dried PNIPAM sample underwent swelling, polymerizing, and washing process analogous to OHA in 1.3, then store at 5 °C.

Synthesis of 1-Pyrenylmethyl Acrylate (PyMA) as Fluorescent Dye: PyMA was synthesized as previously reported.^[30] Solution containing 1-pyrene butyric acid (1 g, 3.47×10^{-3} mol), DMAP (0.08 g, 6.24×10^{-4} mol) and dichloromethane (100 mL) was mixed thoroughly. EDCL was added in a nitrogen environment at 0 °C. The mixture was stirred at room temperature for 1 h, and HEMA (0.45 g, 3.45×10^{-3} mol) was added dropwise at 0 °C. The reaction was then brought to room temperature and stirred for 40 h. The product was diluted with dichloromethane and extracted with 0.02 M hydrochloric acid three times. The organic layer was then dried over sodium sulfate, filtered, recrystallized from methanol, and dried in a vacuum for three days.

Tests of Actuation Behavior: Samples were hung in a glass tube that open at two sides, and the upper side of the tube was connected to a funnel. Liquids with different temperatures were injected into funnel alternately by a syringe subjected to the pump. During heating and cooling, liquids were injected continuously until the tested sample reached a stable length. The entire actuation process was recorded by a camera of 25 fps, measuring the responsive time and strain. Water and *n*-hexadecane were both used to investigate the difference between OHA and HA.

Isometric Contraction Tests For Actuation Strength: The tested sample was fixed by clamps, with one side stuck to the dynamometer and the other side stuck to a large vessel, as Figure 3b. Hot water was poured into vessel to induce volume phase transition. It was observed that OHA preserve a constant volume in the experiment, and HA displayed water loss from the side. The output force underwent a rapid increasing process and a sluggish decreasing process, and the peak value was recorded as the actuation strength.

Periodical Actuation Tests: The sample was hung inside an electrothermal tube, which was connected to a programmable direct current supply, in the water of 15 °C. Voltage was switched between 60 and 0 V to change temperature alternately, and the time for a single cycle varies with sample size (determined by the time required to heat the sample, 19 s for experiment in Figure 3g). The actuation behavior was recorded by camera as stated above, and the periodical force curve was obtained by a dynamometer.

Confocal Laser Scanning Microscope (CLSM) Experiment: For characterization in Figure S2 (Supporting Information), samples were dyed with DAPI (0.01 wt.% to monomer), which was added to the pre-polymerized solution of PNIPAM hydrogel. For characterization in Figure 4a and Figure S10 (Supporting Information), oleophilic phase was dyed by PyMA, which was added to a pre-polymerized solution of PLMA and copolymerized. Hydrophilic phase was dyed by ANSA, which was imported by solvent exchange: OHA was immersed in ANSA solution (3 wt.%) for 24 h at a dark place. All samples were performed on Olympus FV1000-IX81.

Supporting Information

Supporting Information is available from the Wiley Online Library or from the author.

Acknowledgements

The authors appreciate all members of the lab for the support and thank J.Z. for the comments on the final manuscript. This research was supported by the National Key R&D Program of China (2017YFA0207800) and the National Natural Science Funds for Distinguished Young Scholar (21725401).

Note: Figure 1 was revised on March 2, 2023, after initial publication online. In the new version of Figure 1d, the actuation strengths of the traditional volume-phase-transition hydrogel and organohydrogel actuators (high/low) are corrected. The high and low were reversed on initial Early View publication.

Conflict of Interest

The authors declare no conflict of interest.

Data Availability Statement

The data that support the findings of this study are available from the corresponding author upon reasonable request.

Keywords

artificial muscle, muscle-mimicking, organohydrogels, phase transitions, soft confinement

Received: March 9, 2022

Revised: December 11, 2022

Published online: January 5, 2023

- [1] K. Y. Lee, D. J. Mooney, *Chem. Rev.* **2001**, *101*, 1869.
- [2] S. Y. Chin, Y. C. Poh, A. C. Kohler, J. T. Compton, L. L. Hsu, K. M. Lau, S. Kim, B. W. Lee, F. Y. Lee, S. K. Sia, *Sci. Rob.* **2017**, *2*, 6451.
- [3] R. F. Shepherd, F. Ilievski, W. Choi, S. A. Morin, A. A. Stokes, A. D. Mazzeo, X. Chen, M. Wang, G. M. Whitesides, *Proc. Natl. Acad. Sci. USA* **2011**, *108*, 20400.
- [4] Y. S. Kim, M. Liu, Y. Ishida, Y. Ebina, M. Osada, T. Sasaki, T. Hikima, M. Takata, T. Aida, *Nat. Mater.* **2015**, *14*, 1002.
- [5] Z. Pei, Y. Yang, Q. Chen, E. M. Terentjev, Y. Wei, Y. Ji, *Nat. Mater.* **2014**, *13*, 36.
- [6] C. S. Haines, M. D. Lima, N. Li, G. M. Spinks, J. Foroughi, J. D. W. Madden, S. H. Kim, S. Fang, M. J. Andrade, F. Göktepe, O. Göktepe, S. M. Mirvakili, S. Naficy, X. Lepró, J. Oh, M. E. Kozlov, S. J. Kim, X. Xu, B. J. Swedlove, G. G. Wallace, R. H. Baughman, *Science* **2014**, *343*, 868.
- [7] D. J. Beebe, J. S. Moore, J. M. Bauer, Q. Yu, R. H. Liu, C. Devadoss, B. H. Jo, *Nature* **2000**, *404*, 588.
- [8] Y. Takashima, S. Hatanaka, M. Otsubo, M. Nakahata, T. Kakuta, A. Hashidzume, H. Yamaguchi, A. Harada, *Nat. Commun.* **2012**, *3*, 1270.
- [9] A. S. Gladman, E. A. Matsumoto, R. G. Nuzzo, L. Mahadevan, J. A. Lewis, *Nat. Mater.* **2016**, *15*, 413.
- [10] E. Sato Matsuo, T. Tanaka, *J. Chem. Phys.* **1988**, *89*, 1695.
- [11] W. R. K. Illeperuma, J. Y. Sun, Z. Suo, J. J. Vlassak, *Soft Matter* **2013**, *9*, 8504.
- [12] W. R. Frontera, J. Ochala, *Calcified Tissue Int.* **2015**, *96*, 183.
- [13] Z. A. Podlubnaya, in *Structure and Dynamics of Confined Polymers*, NATO Science Partnership Subseries: 3, (Ed.: J. Kasianowicz) Vol. 87, Kluwer Academic Publishers, Amsterdam, The Netherlands **2002**, pp. 295–309.
- [14] T. Luomala, M. Pihlman, *A Practical Guide to Fascial Manipulation*, Elsevier, Amsterdam, The Netherlands **2017**.
- [15] X. Z. Zhang, X. D. Xu, S. X. Cheng, R. X. Zhuo, *Soft Matter* **2008**, *4*, 385.
- [16] R. Yoshida, K. Uchida, Y. Kaneko, K. Sakai, A. Kikuchi, Y. Sakurai, T. Okano, *Nature* **1995**, *374*, 240.
- [17] S. Jiang, F. Liu, A. Lerch, L. Ionov, S. Agarwal, *Adv. Mater.* **2015**, *27*, 4865.
- [18] J. Zhao, H. Su, G. E. Vansuch, Z. Liu, K. Salaita, R. B. Dyer, *ACS Nano* **2019**, *13*, 515.
- [19] H. Gao, Z. Zhao, Y. Cai, J. Zhou, W. Hua, L. Chen, L. Wang, J. Zhang, D. Han, M. Liu, L. Jiang, *Nat. Commun.* **2017**, *8*, 15911.

- [20] M. Shibayama, T. Tanaka, in *Responsive Gels: Volume Transitions I*, (Ed.: K. Dušek) Vol. 109, Springer, Berlin/Heidelberg, Germany **2005**, pp. 1–62.
- [21] T. Binkert, J. Oberreich, M. Meewes, R. Nyffenegger, J. Ricka, *Macromolecules* **1991**, 24, 5806.
- [22] Y. Kaneko, R. Yoshida, K. Sakai, Y. Sakurai, T. Okano, *J. Membrane Sci.* **1995**, 101, 13.
- [23] Y. Liu, K. Zhang, J. Ma, G. J. Vancso, *ACS Appl. Mater. Interfaces* **2017**, 9, 901.
- [24] J. Zhang, K. D. Jandt, *Macro. Rapid Commun.* **2008**, 29, 593.
- [25] L.-W. Xia, R. Xie, X.-J. Ju, W. Wang, Q. Chen, L.-Y. Chu, *Nat. Commun.* **2013**, 4, 12226.
- [26] I. A. Brody, *Exp. Neurol.* **1976**, 50, 673.
- [27] M. Liu, Y. Ishida, Y. Ebina, T. Sasaki, T. Aida, *Nat. Commun.* **2013**, 4, 7532.
- [28] W. Hong, X. Zhao, J. Zhou, Z. Suo, *J. Mech. Phys. Solids* **2008**, 56, 1779.
- [29] Y. Ding, G. Zhang, *Macromolecules* **2006**, 39, 9654.
- [30] K. Kaushlendra, S. Asha, *J. Phys. Chem. B* **2014**, 118, 4951.

ADVANCED MATERIALS

Supporting Information

for *Adv. Mater.*, DOI: 10.1002/adma.202202193

High-Performance Organohydrogel Artificial Muscle
with Compartmentalized Anisotropic Actuation Under
Microdomain Confinement

*Longhao Zhang, Hao Yan, JiaJia Zhou, Ziguang Zhao,
Jin Huang, Lie Chen, Yunfei Ru, and Mingjie Liu**

Supporting Information

High performance organohydrogel artificial muscle utilizing phase transition under soft confinement

Longhao Zhang, Hao Yan, Jiajia Zhou, Ziguang Zhao, Jin Huang, Lie Chen, Yunfei Ru, Mingjie
Liu*

Correspondence to: liumj@buaa.edu.cn

Table of Contents

1. Materials.....	2
2. Instrumentation.....	2
3. Procedures for preparation organohydrogel actuator (OHA).....	3
4. Procedures for actuation strength test.....	4
5. Supplementary Figures (S1-S21).....	6
6. Supplementary Table.....	29
7. Description of Supplementary videos.....	30

1. Materials

Reagents including N-isopropylacrylamide (NIPAM, 98%, GC), lauryl methacrylate (LMA, 95%, GC), 2-hydroxyethyl methacrylate (HEMA, 95%), 4-dimethylaminopyridine (DMAP, 99%), 1-pyrene butyric acid (98%) was purchased from Tokyo Chemical Industry (TCI) and used as received. Acrylamide (AM), ethylene glycol dimethacrylate (EGDMA, 99%), 2,2-diethoxyacetophenone (DEOP, 98%), N, N'-methylene bisacrylamide (BIS), 4', 6-diamidino-2-phenylindole dihydrochloride (DAPI) were purchased from Sigma-Aldrich and used as received. 1-Ethyl-3-(3-dimethylaminopropyl) carbodiimide hydrochloride (EDCL, 98%), N-(1-Naphtyl)-3-aminopropanesulfonic acid sodium salt (ANSA) and solvents including ethanol, acetone, dichloromethane were purchased from Aladdin Biomedical Technology Company. Inorganic nano-clay (Laponite XLS, $[\text{Mg}_{5.34}\text{Li}_{0.66}\text{Si}_8\text{O}_{20}(\text{OH})_4] \text{Na}_{0.66}$, MW= 762.24, layer size = 20-30 nm in diameter and 1 nm in thickness) was purchased from Rockwood Ltd., UK

2. Instrumentation

Tension. Tensile stress-strain experiments were performed on SUNS UTM4000 instrument at room temperature (25°C). Tensile bar (50mm × 10mm × 1mm) was prepared by laser cutting of OHA. Unless otherwise noted, tensile speed was utilized as 10 mm/min. Each sample was repeated three times to obtain a statistical result.

Rheological tests. The dynamic viscoelasticity of the PLMA was measured by an Anton Paar model MCR-302 rheometer. The samples were placed under a 15 mm-diameter parallel plate. Storage moduli (G') and loss moduli (G'') was measured by frequency sweep tests, in which the angular frequency (ω) ranging from 0.1 rad/s to 100 rad/s with the shear strain (γ) of 0.5% and 25 °C.

Confocal laser scanning microscope (CLSM). In CLSM experiments, all samples were performed on Olympus FV1000-IX81. When simply marked hydrophilic phase (Fig. S2), samples were dyed with DAPI (0.01 wt.% to monomer), which was added to the pre-polymerized solution of PNIPAM hydrogel. For characterization in Fig. 4a and Fig. S10, oleophilic phase was dyed by PyMA, which was added to pre-polymerized solution of PLMA and copolymerized. Hydrophilic phase was dyed by ANSA, which was imported by solvent exchange: OHA was immersed in ANSA solution (3 wt.%) for 24 h at dark place. This dying strategy insured the phase transition process could be characterized. Here the hydrophilic networks were tested by lasers with the wavelength of 405 nm, and oleophilic networks were tested by lasers with the wavelength of 488 nm. Laser strength were adjust carefully until overexposure and dark-background were eliminated thoroughly.

Differential scanning calorimetry (DSC). DSC experiments were performed on Mettler-Toledo DSC 3. Samples were cut into pieces with weight of ~ 10 mg, and set in aluminum crucible for experiment. Temperature was ranging from 15 °C to 50 °C, at rate of 5 °C/min. The sample was heated twice and utilized the secondary heating as result, in order to eliminate the thermal history.

Fourier transform infrared (FTIR). FTIR experiments were conducted on a Bruker Vertex 80V with ATR module at 25 °C. Samples were washed with ethanol to clean the surface, and tested directly. The obtained curves were focused on wave number around 3300 cm^{-1} to observe the transformation of C=O radical.

3. Procedures for preparation organohydrogel actuator (OHA)

The preparation of OHA is the most important fabrication process, which was displayed in Fig. S1. PNIPAM hydrogels crosslinked with XLS nano-clay were first prepared, stretched and dried. Pre-polymerized solution for oleophilic network was prepared by mixing LMA (monomer), DEOP (photo-initiator), EGDMA (cross-linker) and 100 mL of ethanol (solution). Here we control the

concentration of LMA to adjust oleophilic to hydrophilic network ratio, which was detailed summarized in Table S1. Since the incorporated monomers could not be polymerized thoroughly, the obtained network ratio is not in direct proportion to monomer concentration. The concentration of DEOP is 0.01 *wt.%*, and concentration of EGDMA is 0.5 *wt.%* (both are the mass fraction to LMA). Dried PNIPAM was swelled with prepared solution (in fixed state) for 4 h at cool, dark place. Obtained thoroughly swelled PNIPAM was polymerized by ultra-violet (365 nm) for 30 mins at room temperature. The sample was washed by ethanol and water alternately for three times to remove unreacted monomers, then swelled in water for 12 h (change water at least three times) until exchanged solvent completely. To measure m_{ON} (ON refers to oleophilic network), sample should be dried and weighted after washed and before swelled in water, and m_{ON} can be calculated as follow:

$$m_{ON} = m_{\text{measured}} - m_{HN}$$

Here m_{ON} and m_{HN} are utilized to measure oleophilic to hydrophilic network ratio. OHA was store at 5 °C for later use.

4. Procedures for actuation strength test

Actuation strength is an important index for artificial muscle but is less characterized in hydrogel actuators, commonly owing to their weakness. Here we utilized the method originated from the isometric contraction of muscle, as described in Fig. S8. The output forces of muscles increase followingly when adding load, whereas their strokes decrease. The maximum actuation strength was obtained when stroke reached zero, here the actuation strength could be regarded as an index for actuators. We designed test devices for hydrogel actuators based on above mechanism.

Tested sample was fixed by clamps, with one side stick to dynamometer and the other side stick to a large vessel, as Fig. 3b. Hot water was poured into vessel to induce volume phase transition. We observed that hydrogel actuators display water loss from side because their lengths are fixed, meanwhile OHAs preserve a constant volume. The curves of actuation strength underwent a rapid increasing process and reached the maximum, afterwards a sluggish decreasing process appears (Fig. S9). We suppose the decrease is owing to the fundamental relaxation feature of polymers. As a result, we regard the peak value as the maximum actuation strength, which is utilized in performance comparison.

5. Supplementary Figures (S1-S12)

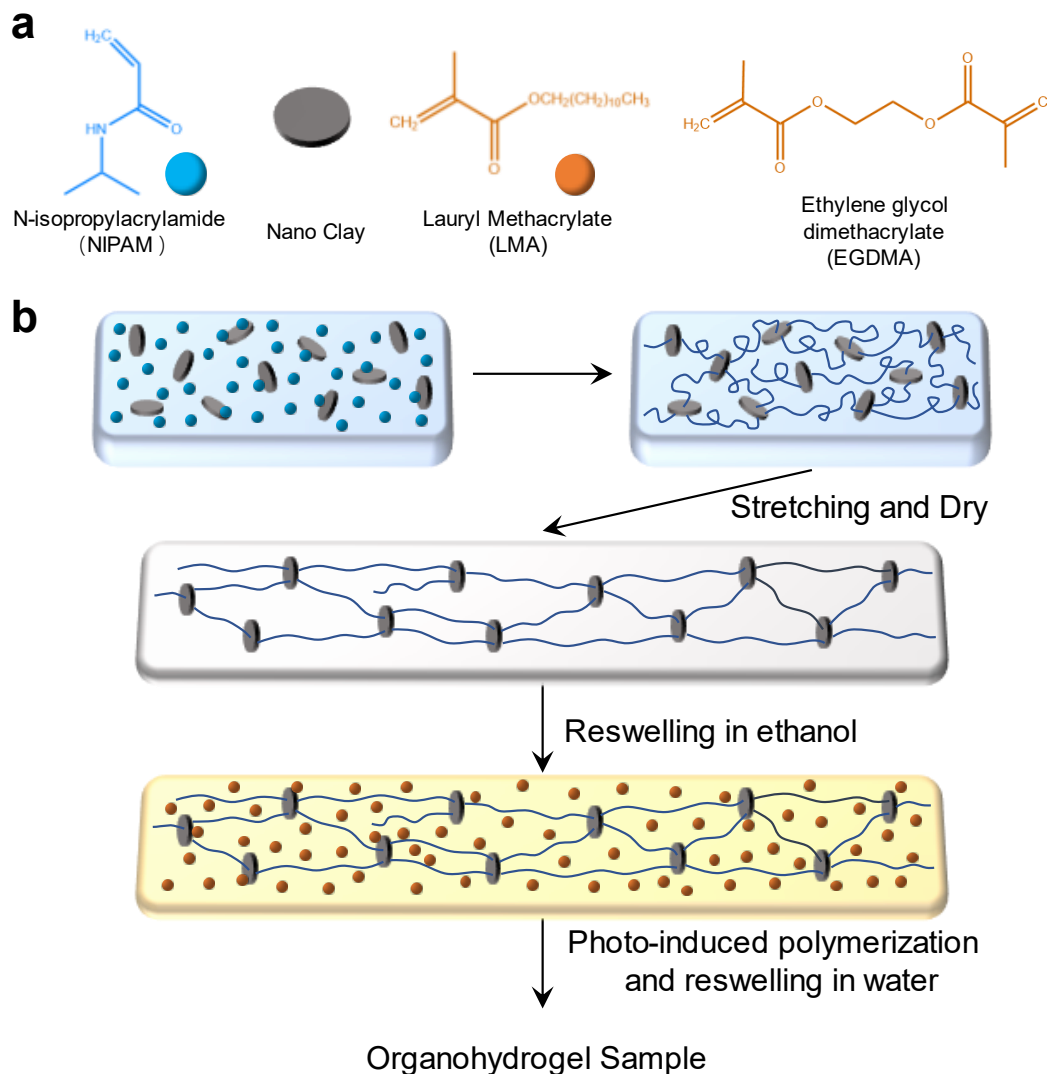


Fig. S1. **a**, Formula of OHA components and detailed fabrication process. **b**, The detailed fabrication process and network state in different solvent. Hydrogels were polymerized at 0 °C, stretched, fixed and dried at 25 °C. The samples were then immersed in the precursors of oleophilic network, and polymerized at 25 °C.

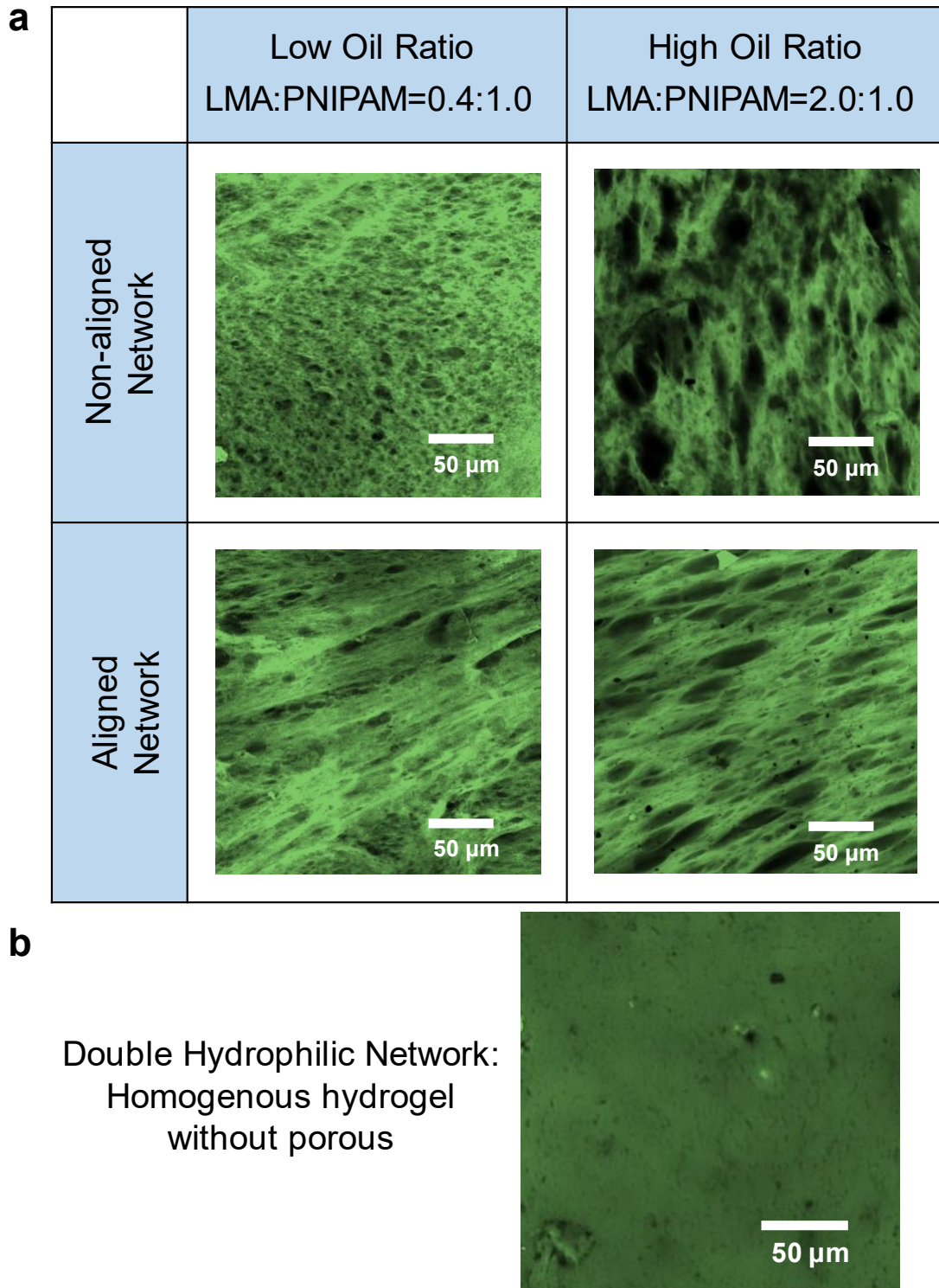


Fig. S2. a, Structure of OHA with different network ratio and orientation degree. **b**, Homogenous HA sample as comparison. All samples were dyed on hydrophilic phase by DAPI, and tested by laser of 405 nm on CLSM.

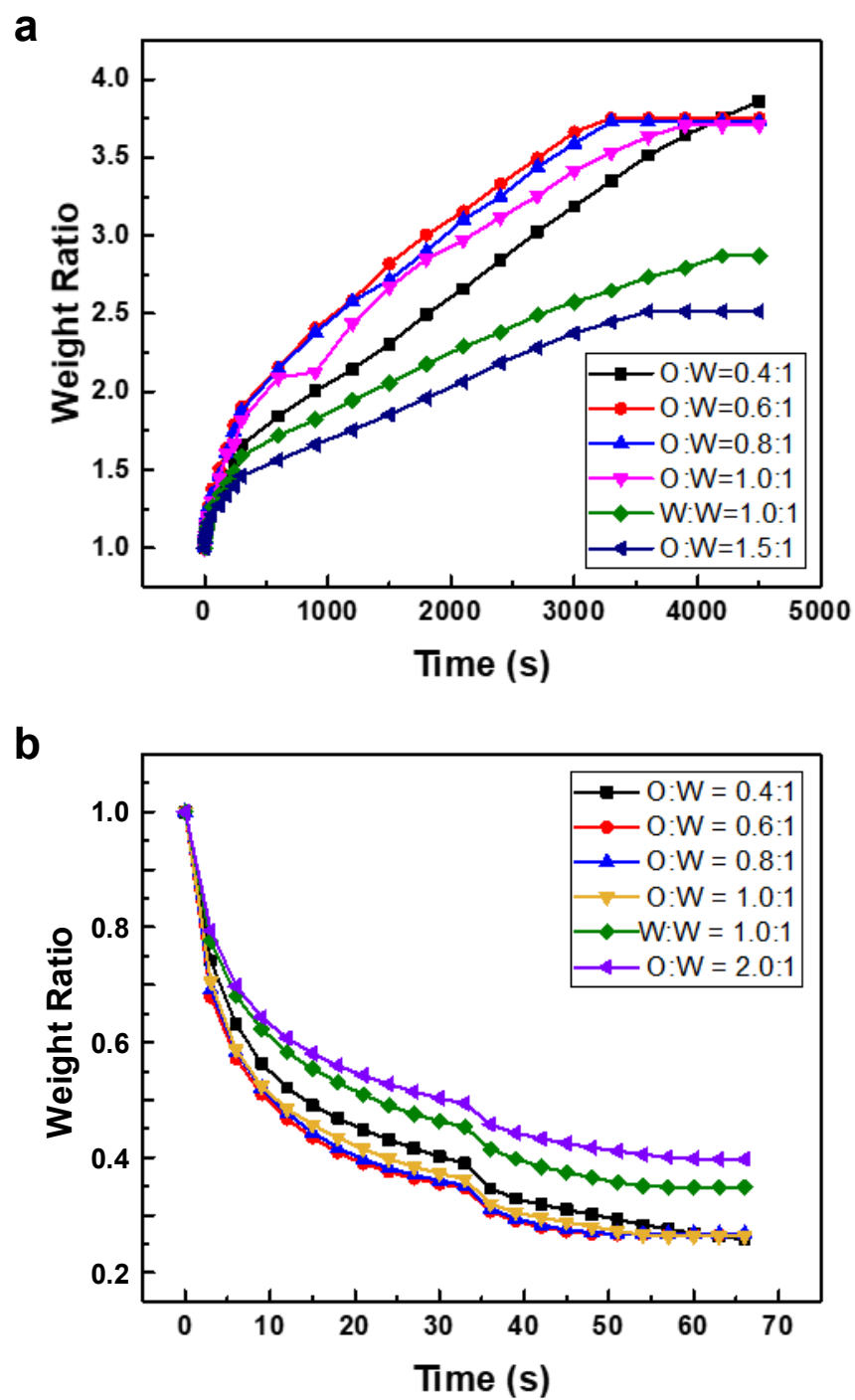


Fig. S3. Swelling (a) and deswelling (b) curves of OHA. All weight are marked as normalization weight ratio, indicate the ratio between current weigh and original weight.

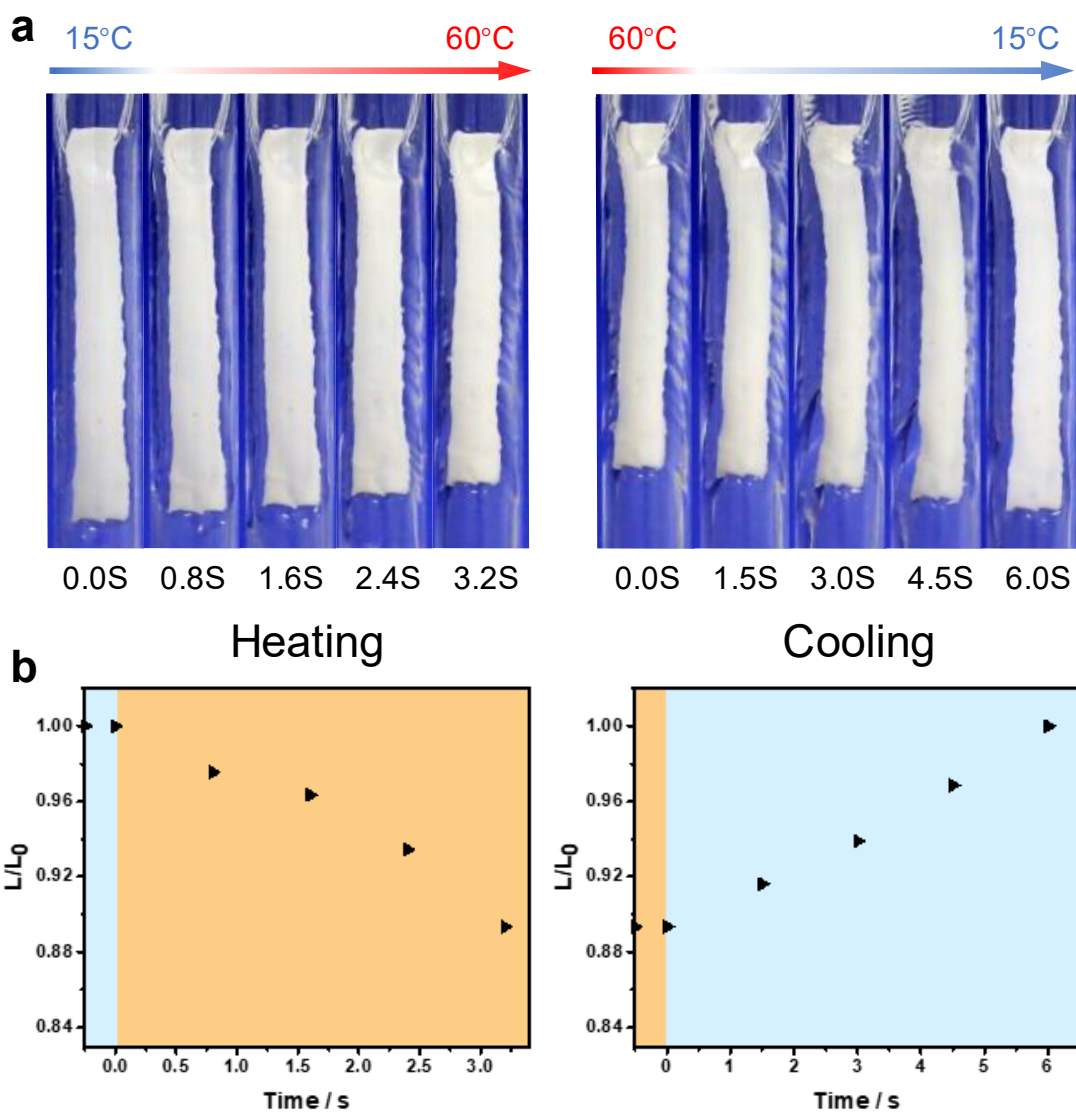


Fig. S4. Actuation and data statistic of OHA in water environment.

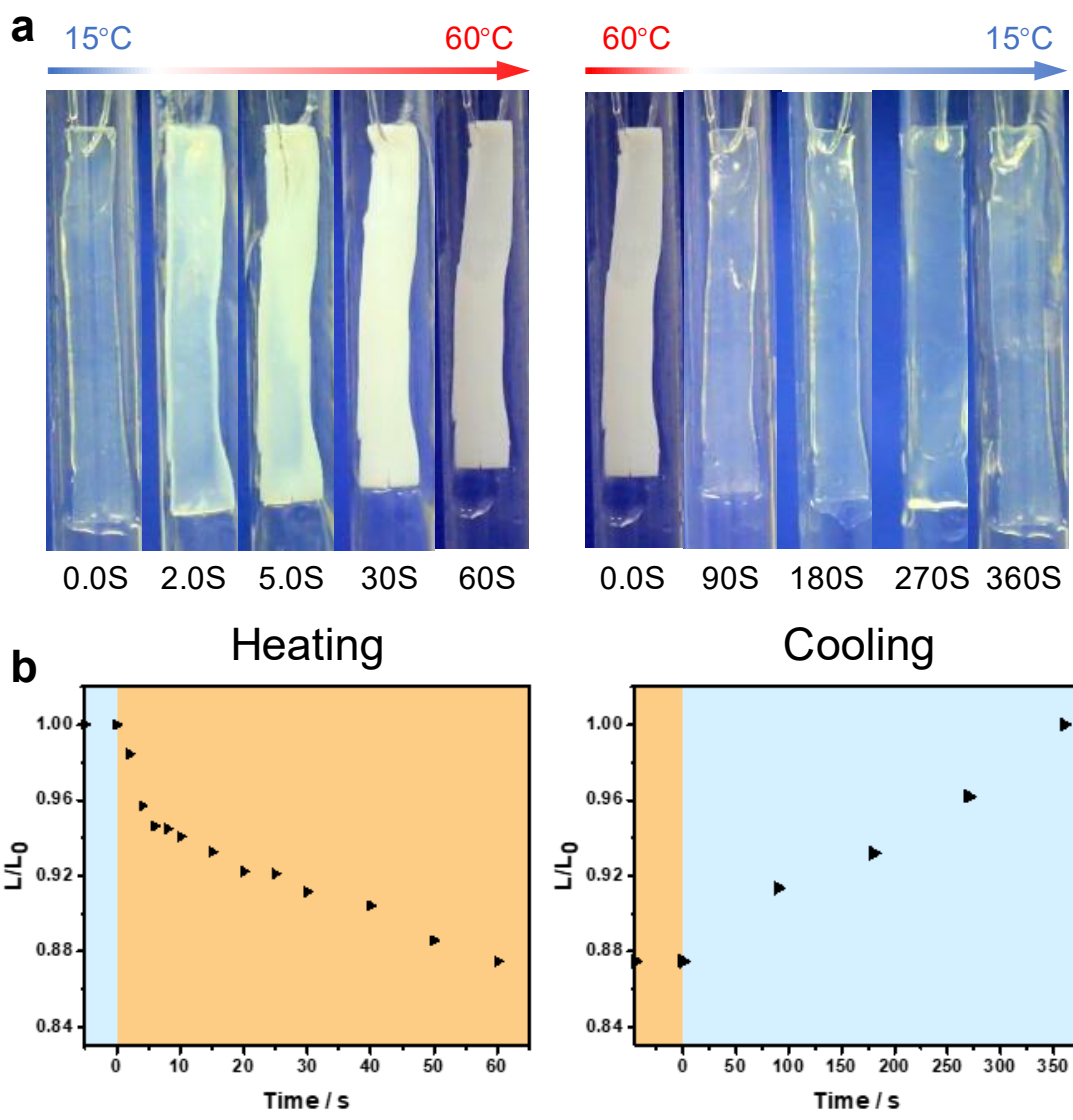


Fig. S5. Actuation and data statistic of HA in water environment.

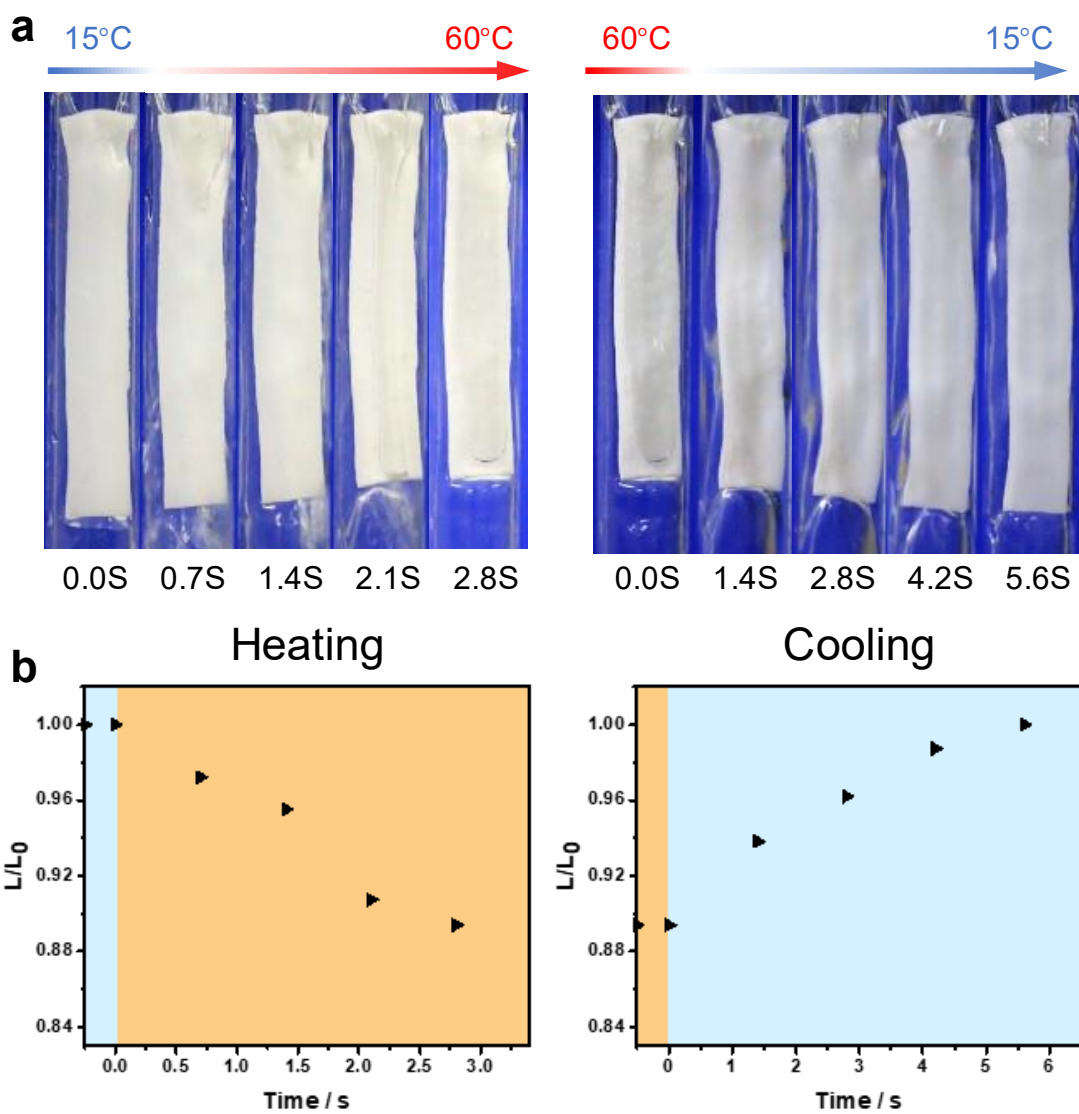


Fig. S6. Actuation and data statistic of OHA in n-hexadecane environment.

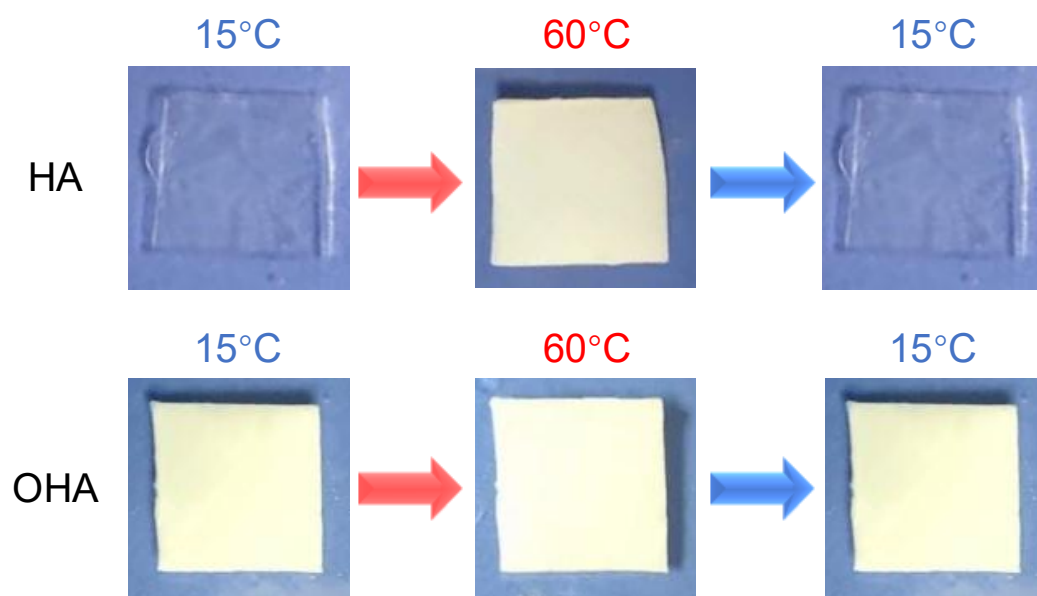


Fig. S7. Non-aligned samples could not deform in response to temperature.

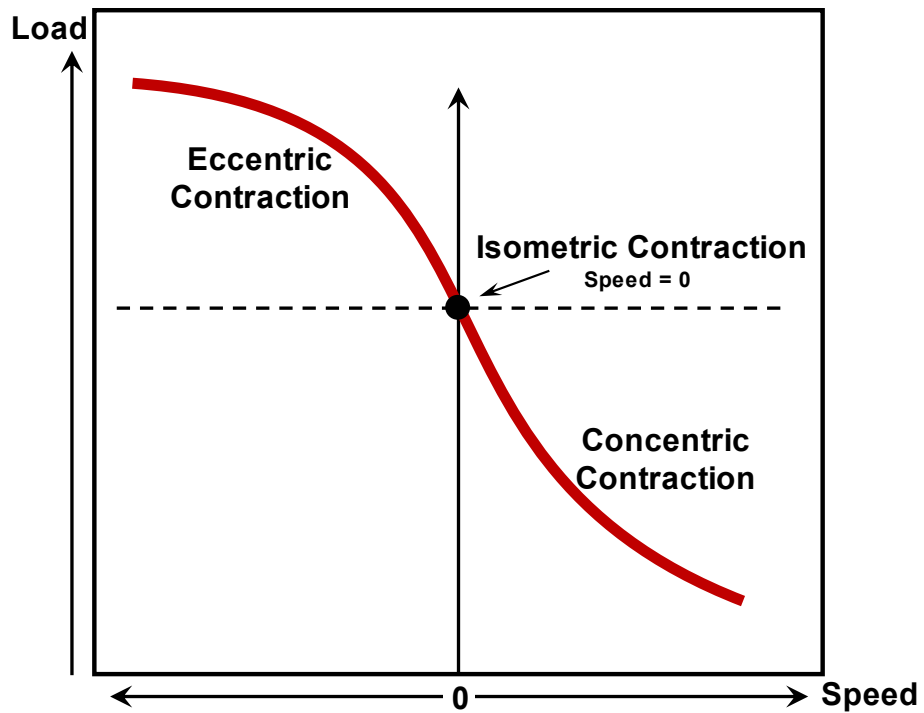


Fig. S8. Different contraction model for skeletal muscle. When loads added gradually, muscle underwent concentric, isometric and eccentric contraction mode in order. Since the load could not be lifted in eccentric contraction mode, the isometric contraction point is regarded as the maximum output force.

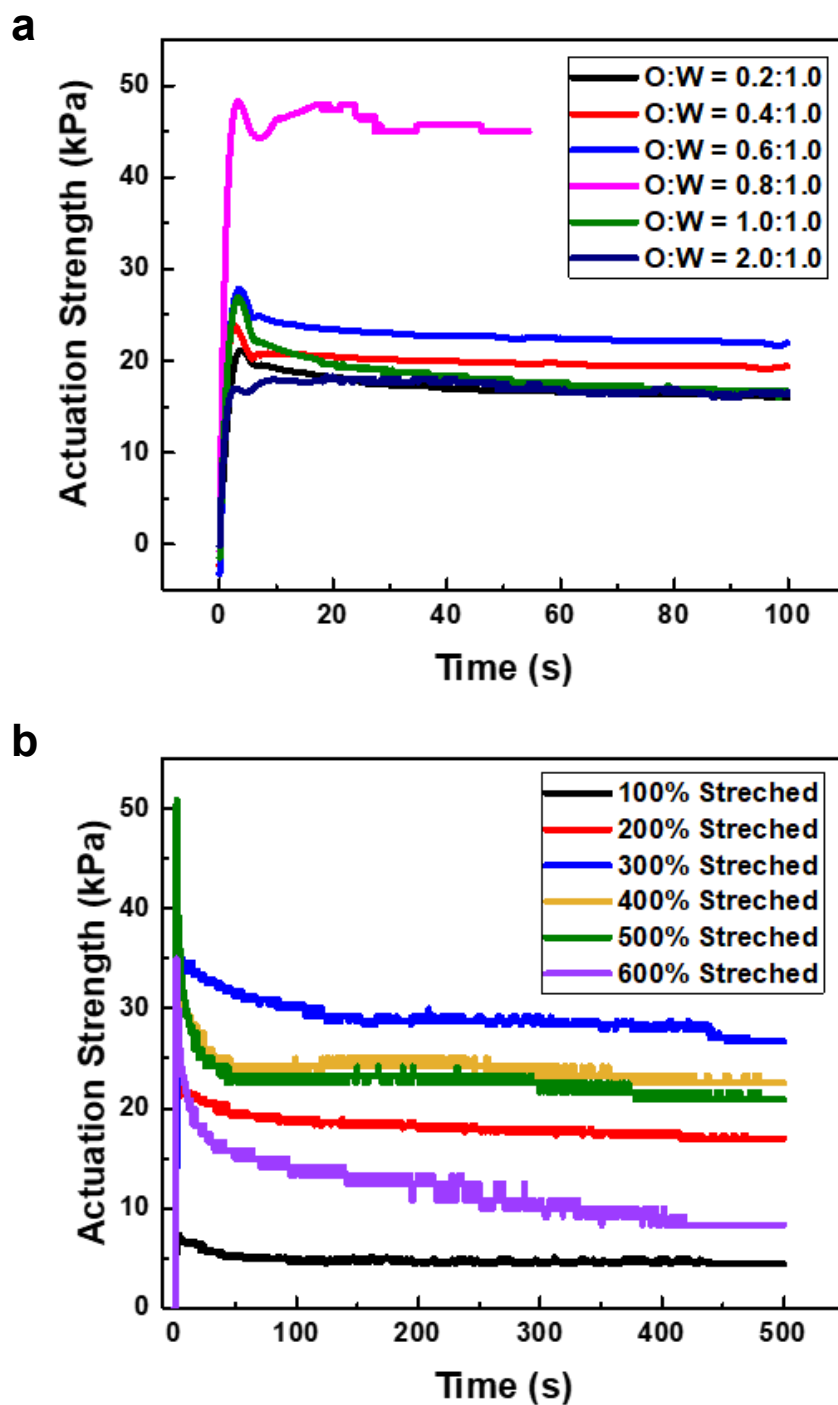


Fig. S9. Actuation strength to time curves after immersed in hot water. The water temperature was set at 60 °C in all experiments. The peak value corresponds to the maximum actuation strength, and the decrease process is originated from relaxation. **a**, samples with different hydrophilic to oleophilic network ratio. **b**, samples with different stretched ratio.

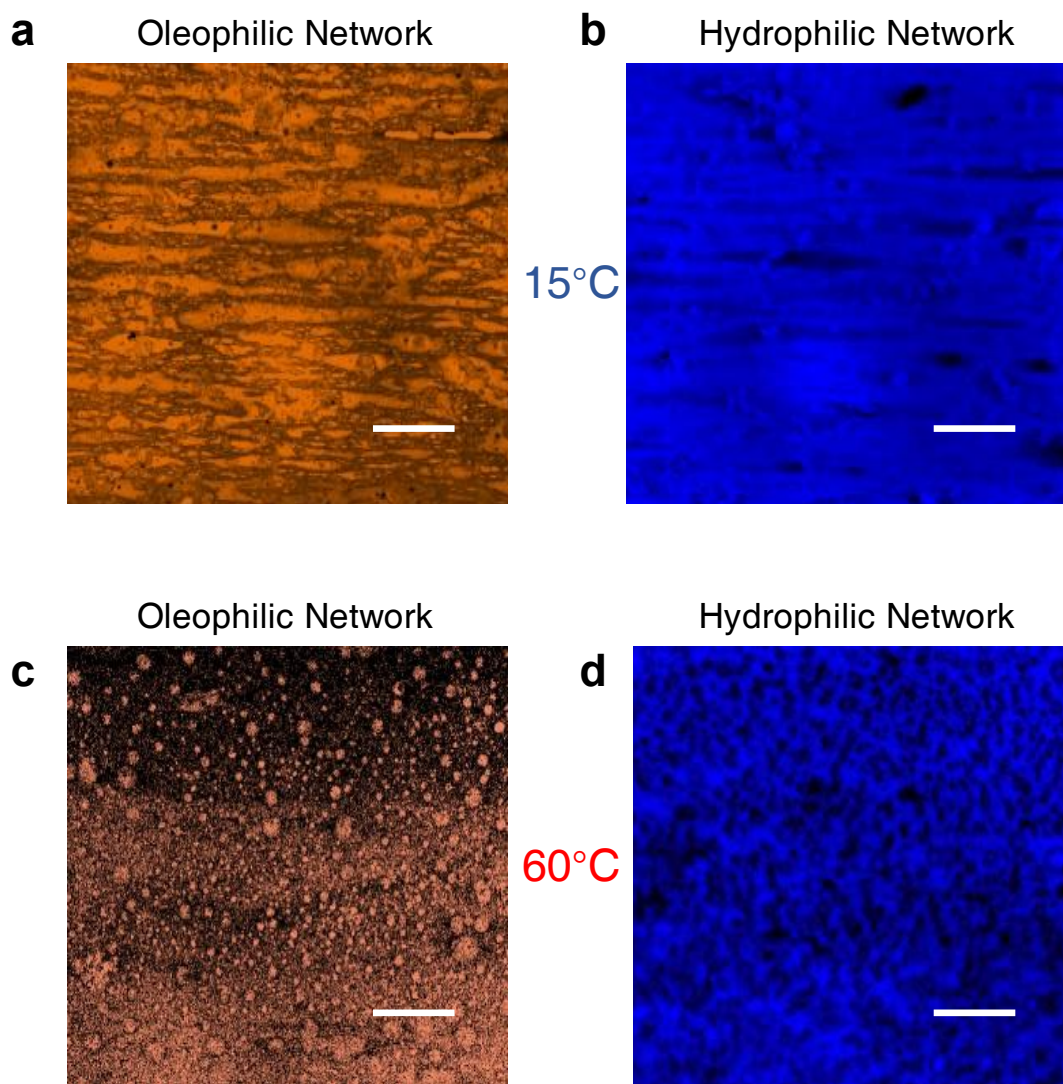


Fig. S10. CLSM images of oleophilic network and hydrophilic network in OHA during phase transition. **a**, Oleophilic network at 15 °C. **b**, Hydrophilic network at 15 °C. **c**, Oleophilic network at 60 °C. **d**, Hydrophilic network at 60 °C. In all samples, hydrophilic networks were dyed by ANSA and test by laser with 405 nm; oleophilic networks were dyed by PyMA and test by laser with 488 nm.

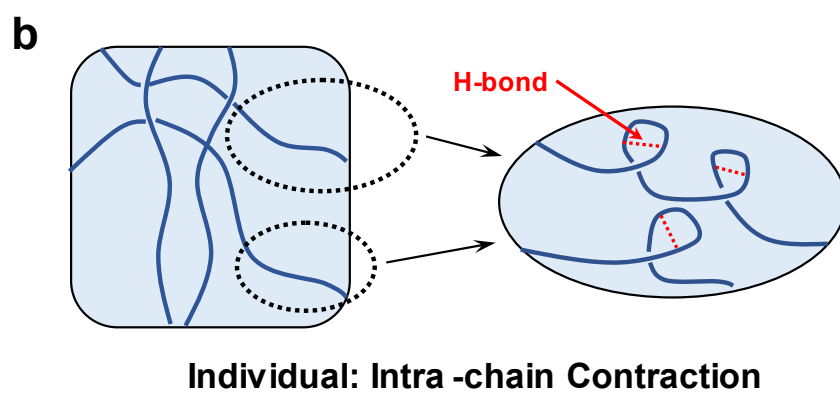
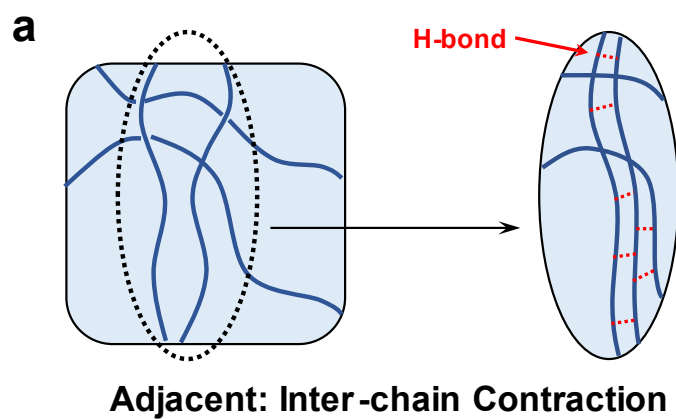


Fig. S11. Scheme of inter-chain (a) and intra-chain (b) contraction model of PNIPAM. Since inter-chain H-bond is more stable, PNIPAM networks prefer to aggregate during phase transition. The individual network ratio was increased in OHA because the isolation effect of oleophilic networks, thus undergoing intra-chain contraction.

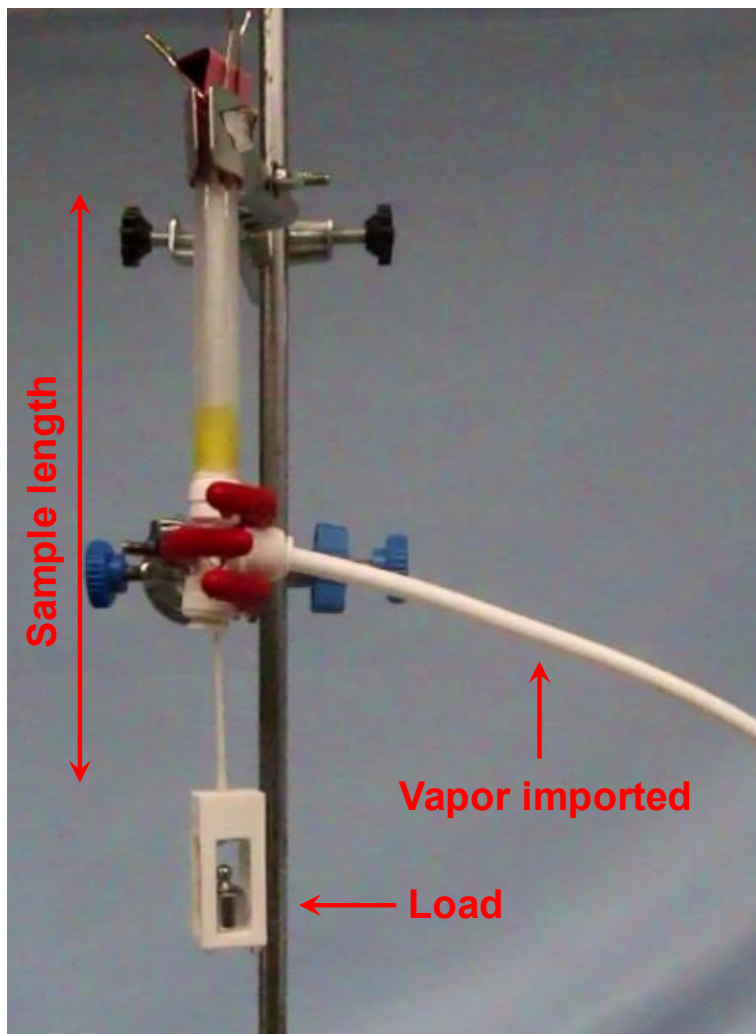


Fig. S12. Illustration of demonstration experiment. A 0.2 g sample placed in a tube, and water vapors were imported persistently to heat the sample and induce actuation. Here loads of 17.1 g could be lifted.

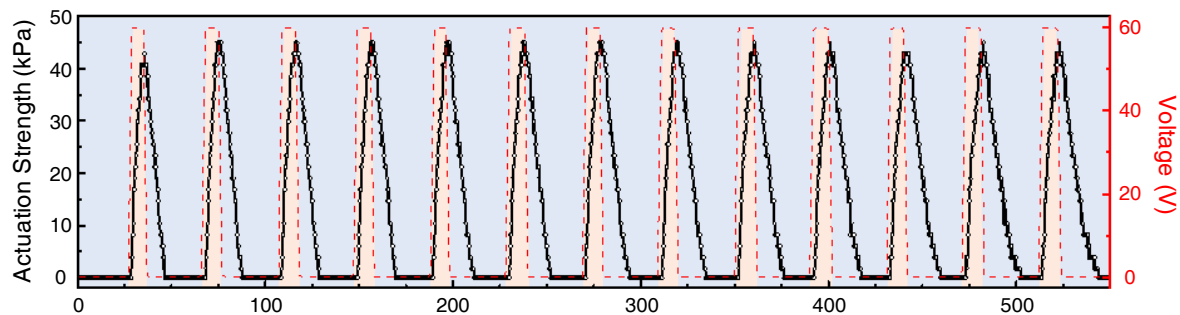


Figure S13. Circulation experiment of OHA_{0.8-1.0-4}. Samples were immersed in water with 15 °C and tangled with electrothermal coils. Electrothermal coils were connected to a programmable DC power, supplying voltage ranging from 0 V - 60 V to heat OHA sample.

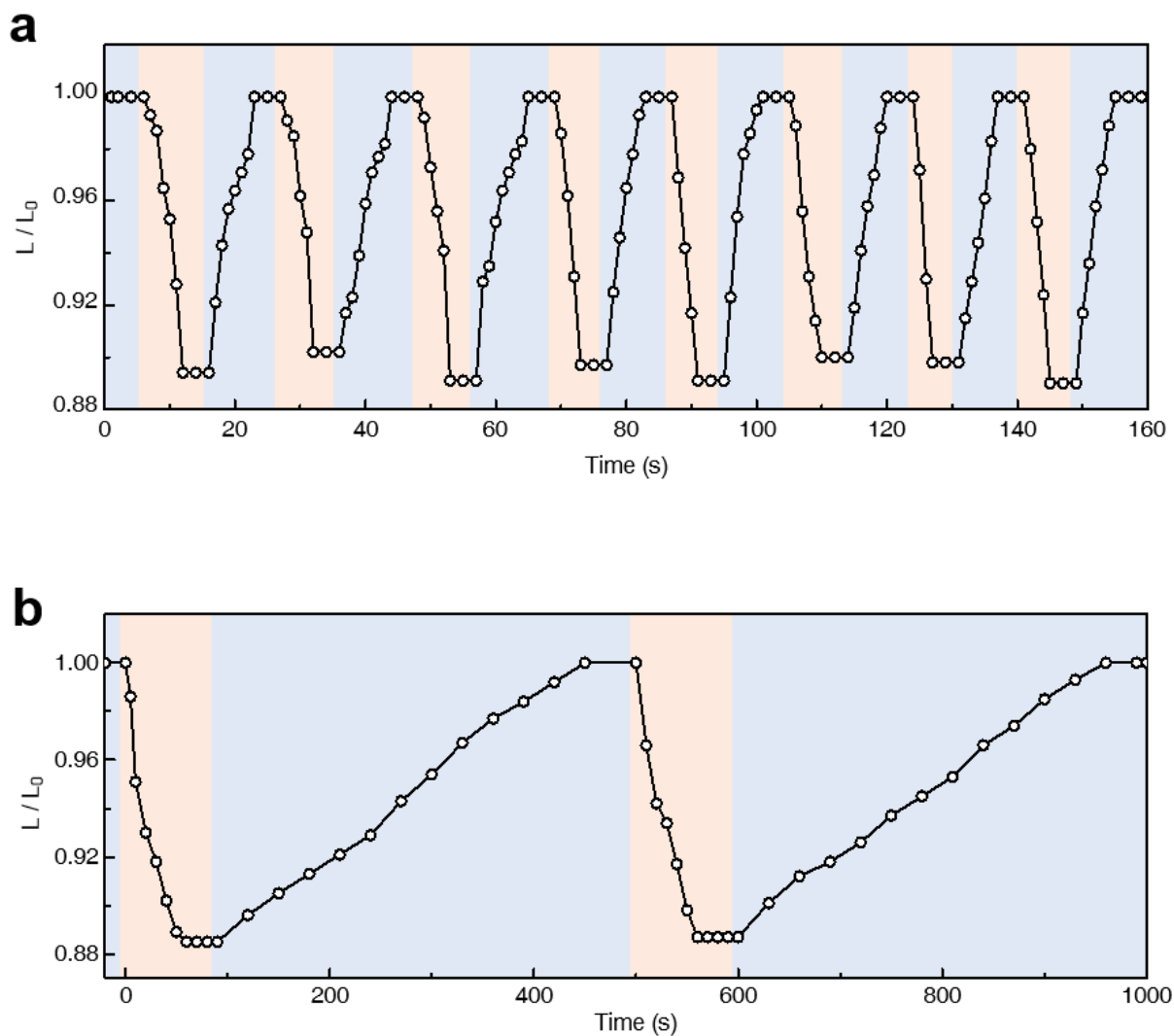


Figure S14. Circulation actuation of organohydrogel actuator (OHA) and hydrogel actuator (HA). Samples were heated and cooled by water at 60°C or 15°C, temperature was changed by pouring hot water or cool water (as temperature above) to control same heating or cooling rate. **(a)** Circulation actuation of OHA. **(b)** Circulation actuation of HA.

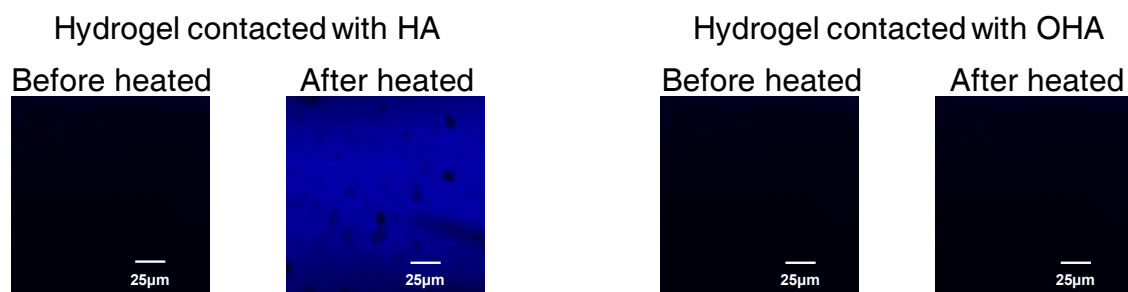


Figure S15. Macroscopically water movement marked by fluorescent label.

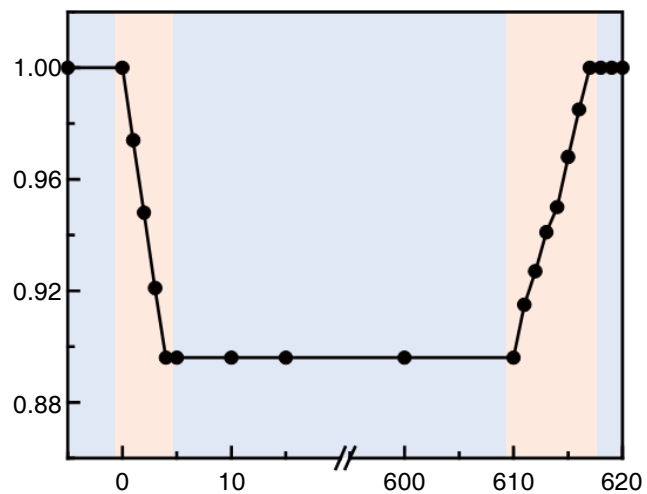


Figure S16. Actuation of OHA in n-hexadecane. OHA sample can recover to its original length even after heated for 600 s.

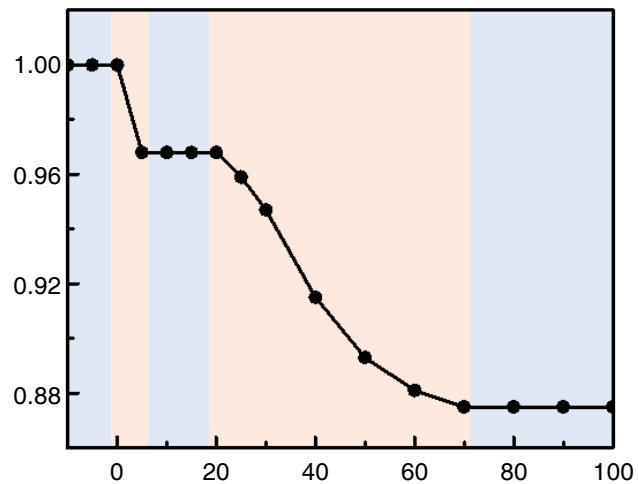


Figure S17. Actuation of HA in n-hexadecane. HA sample cannot recover even under short period of heating.

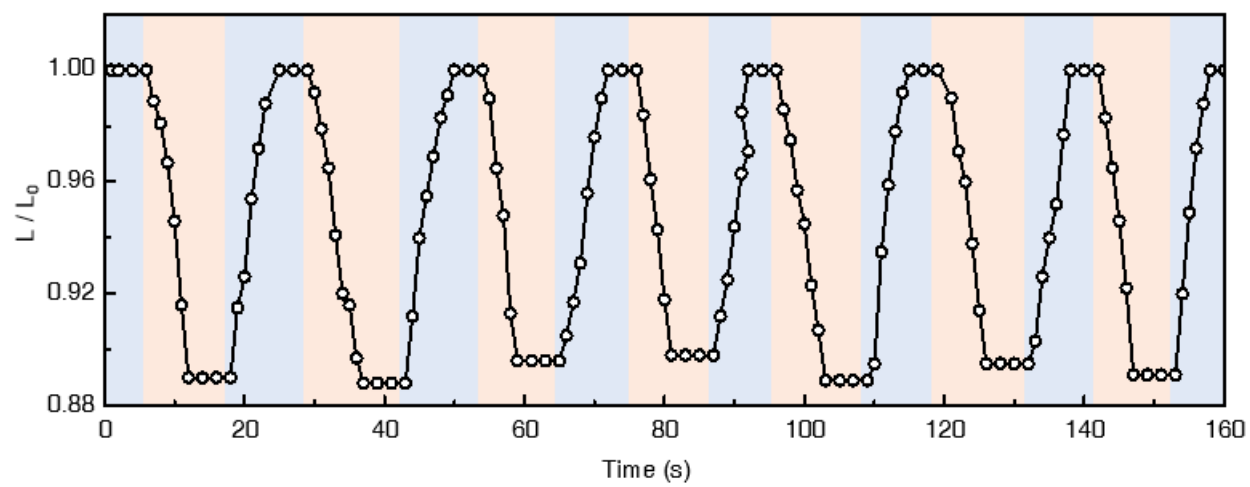


Figure S18. Circulation actuation of OHA in n-hexadecane.

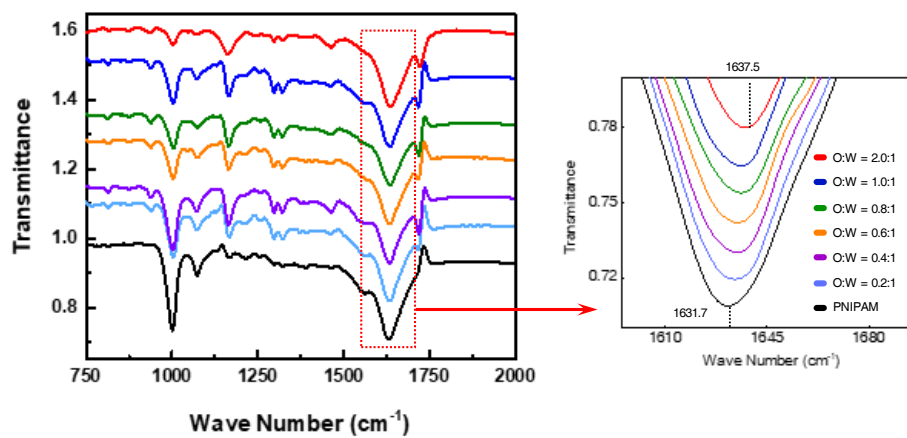


Figure S19. ATR-FTIR spectrum of OHAs at 25 °C and zoom area.

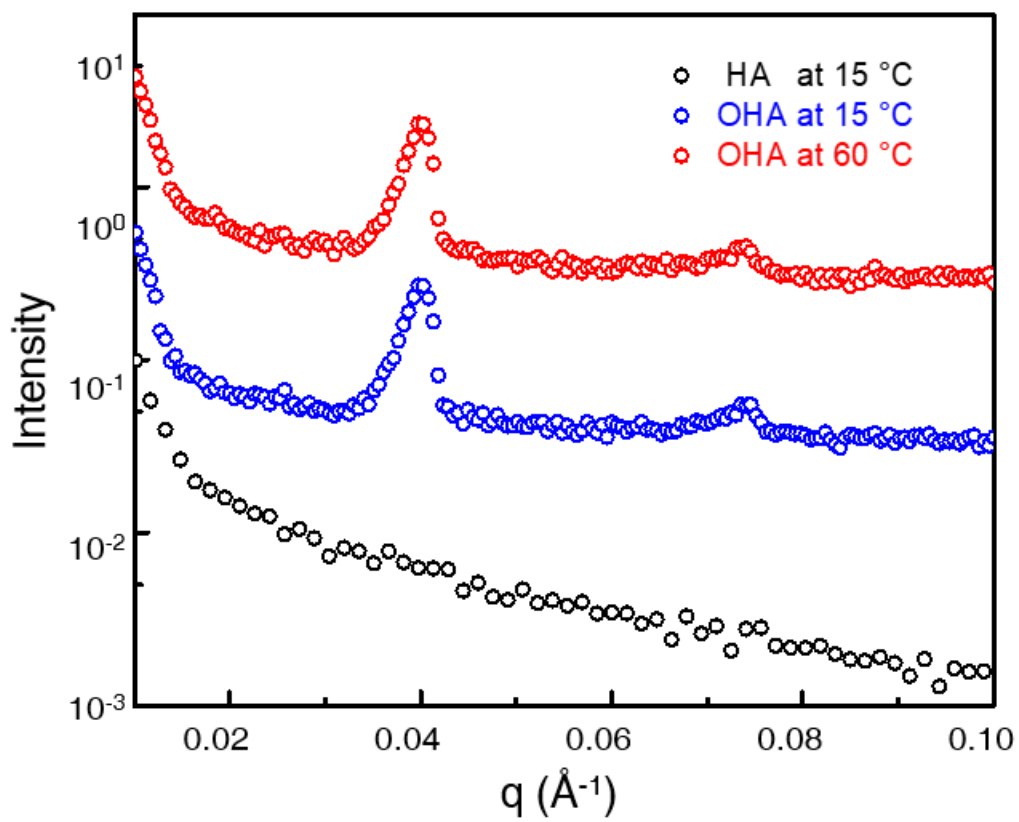


Figure S20. SAXS characterization of OHA and HA.

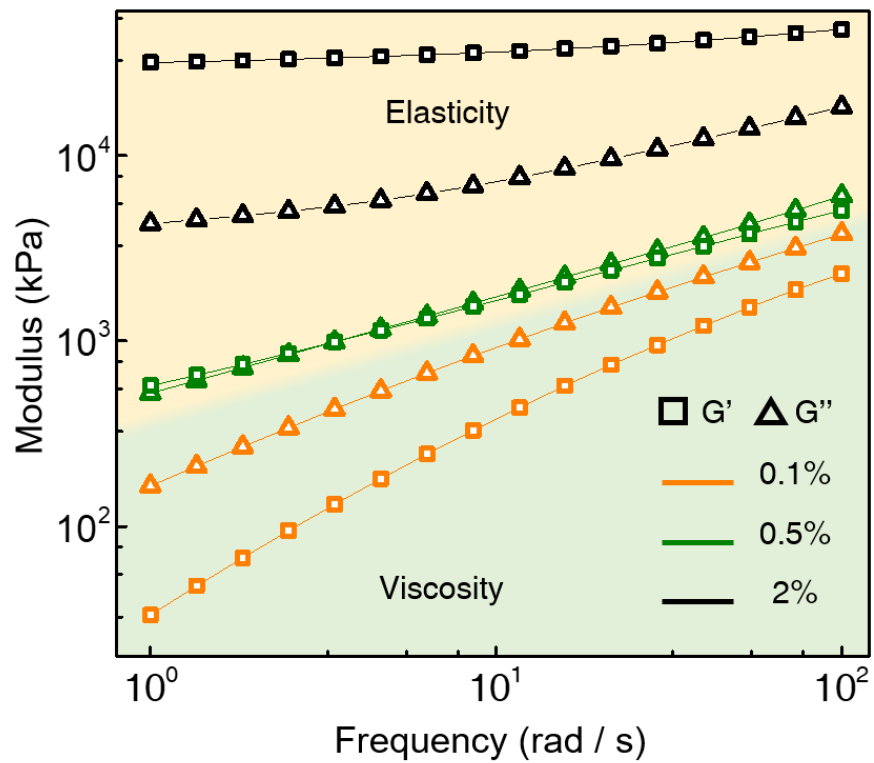


Figure S21. Rheological measurement of OHAs with different crosslinking density.

Frequency was ranged from 1 rad/s to 100 rad/s, with γ of 0.5% at 25 °C

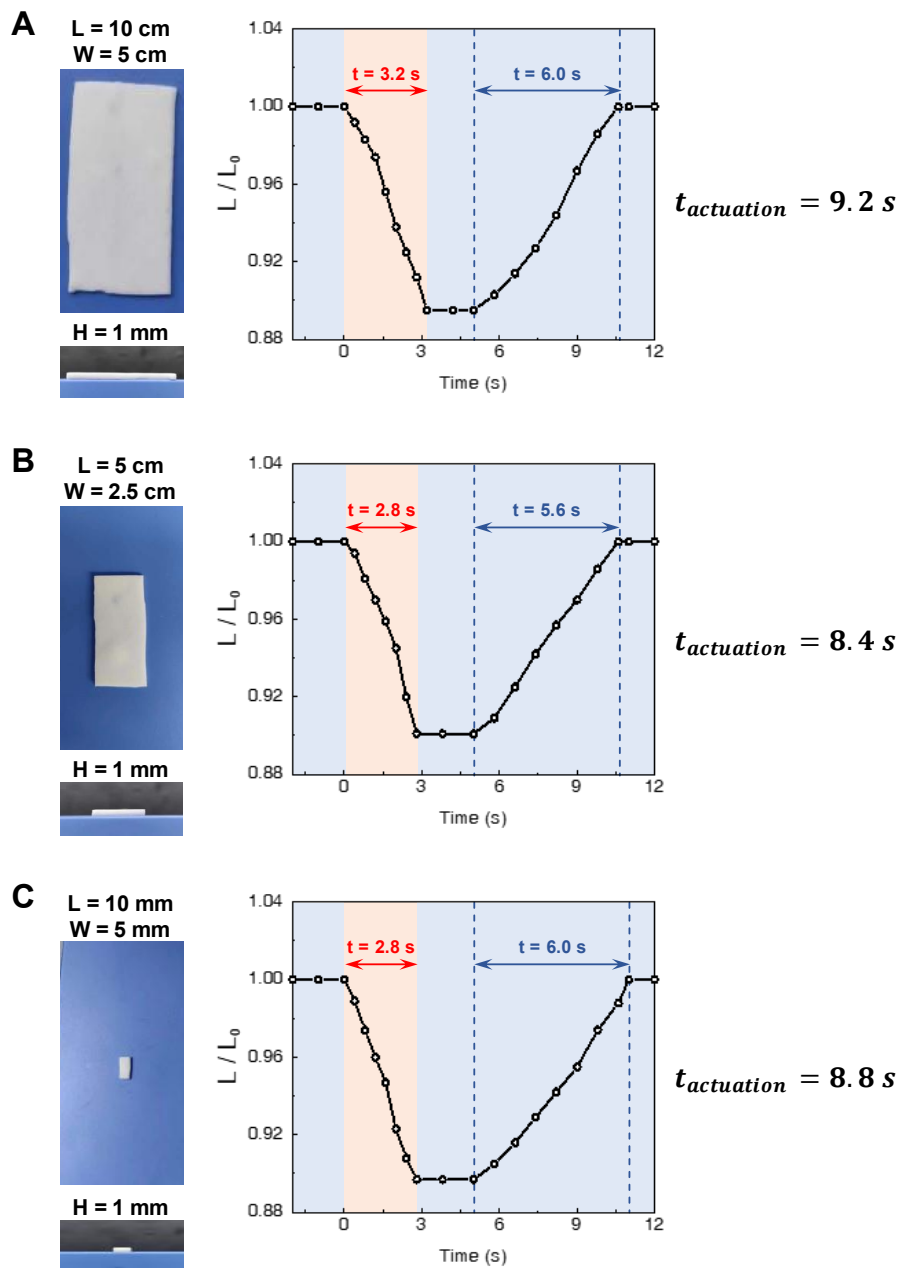


Figure S22. Actuation speed comparison of samples with different surface area. The heights of all samples were kept at 1 mm to obtain same heat transfer speed. **A**, OHA of 10 cm x 5 cm x 1mm. **B**, OHA of 5 cm x 2.5 cm x 1mm. **C**, OHA of 10 mm x 5 mm x 1 mm.

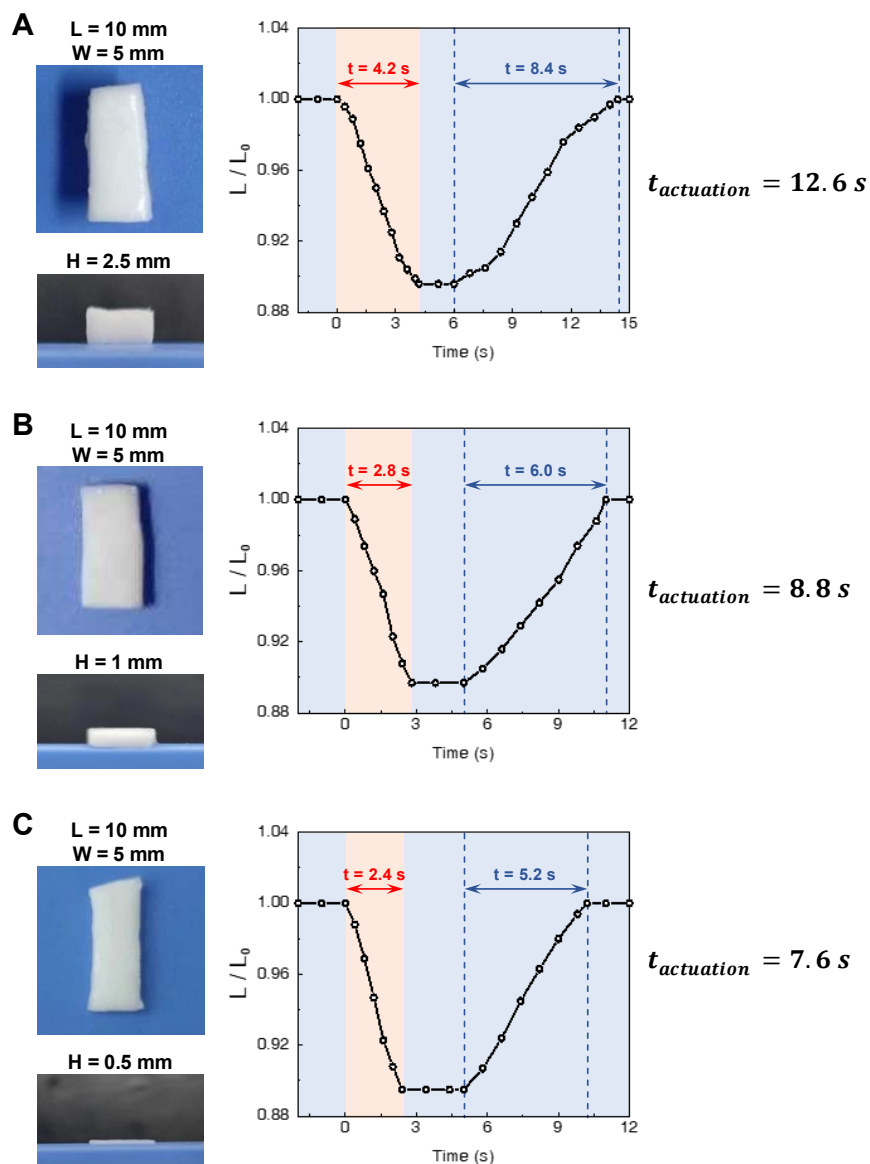


Figure S23. Actuation speed comparison of samples with different height. The surface area of all samples was kept at 10 mm x 5 mm. **A**, OHA with height of 2.5 mm. **B**, OHA with height of 1 mm. **C**, OHA with height of 0.5 mm.

6. Supplementary Table

Table S1. Oleophilic to hydrophilic network ratio controlled by pre-polymerized solution concentration.

PLMA concentration	Oleophilic to hydrophilic network ratio
7 wt.%	0.2 to 1.0
16 wt.%	0.4 to 1.0
22 wt.%	0.6 to 1.0
28 wt.%	0.8 to 1.0
36wt.%	1.0 to 1.0
62 wt.%	2.0 to 1.0

Table S2. The weight comparison of HA and OHA. The original weight of all samples were firstly measured at 15°C. The samples were heated to 60°C to measure the weight after contraction, and then cooled to 15°C to measure the weight after elongation.

Hydrogel Type	HA		OHA	
	Weight	Δ	Weight	Δ
Original	0.2448g		0.2359g	
After contraction	0.2055g	0.0393g, 16.1%	0.2314g	0.0045g, 1.9%
After elongation	0.2413g	0.0358g, 14.8%	0.2349g	0.0035g, 1.5%

7. Description of Supplementary videos

Movie S1.

A supporting movie showing the actuation process of OHA in water, with temperature changing from 15 °C to 60 °C circularly.

Movie S2.

A supporting movie showing the actuation process of OHA in n-hexadecane, with temperature changing from 15 °C to 60 °C circularly.